Active Wing Shaping Control Concept Using Composite Lattice-based Cellular Materials

ARC: Sean Swei (PI), Kenny Cheung (Co-I), Nick Cramer (UCSC), Nhan Nguyen, Benjamin Jenett (MIT), Daniel Cellucci (Cornell) Robert Nakamura

LaRC: Mike Fremaux, Mark Croom, Mia Siochi, Wes Oneal, Clinton Duncan, Lee Pollard, Earl Harris, Sue Grafton, Gary Wainwright

MIT/CBA: Prof. Neil Gershenfeld, Sam Calisch, Dick Perdichizzi

NASA Aeronautics Research Mission Directorate (ARMD)

2015 LEARN/Seedling Technical Seminar

January 13–15, 2015

Project Objectives

- Develop a novel aerostructure concept by combining the advanced composite lattice-based cellular materials/ components and the multi-objective optimal flight control systems to realize mission adaptive and aerodynamically efficient air vehicles
- The goal is to utilize the "*building block*" strategy for lattice-based components to enable high "stiffness-to-density" ratios; large Young's modulus for an ultra-light material, and provide great adaptability for varying flight scenarios

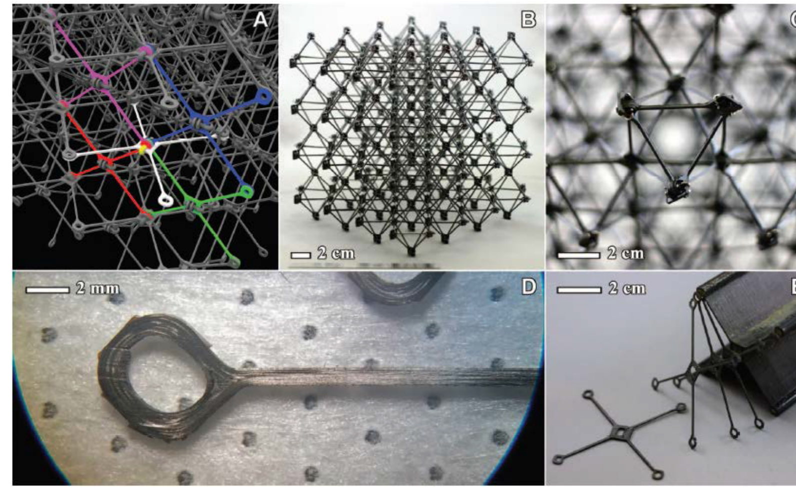

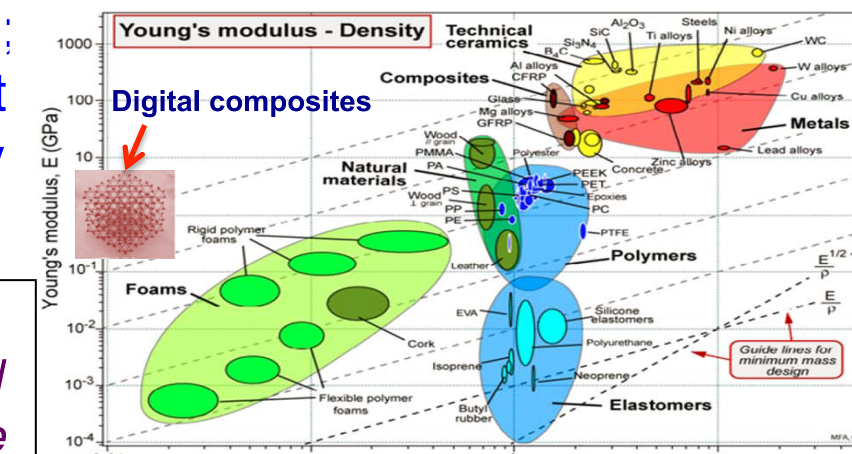

Aircraft industries are beginning to explore the potential use of digital composite materials and manufacturing in aircraft construction to reduce weight and construction/assembly costs.

kenny@nasa.gov

Innovation of Research

- Aim to take advantage of an emerging manufacturing method based on micro-lattice structures to build a topologically optimized aerostrcture with digital composite materials that enables *variable stiffness* control surfaces
- The developed platform will be used to *assess* the aerodynamic and aeroelastic benefits of morphing wing configurations compared to conventional airframe designs
- The aerostructure needs to be sufficiently robust to be evaluated in wing tunnel tests to determine the stability of such a reconfigurable structure to maintain the necessary shapes for optimal performance across flight envelop

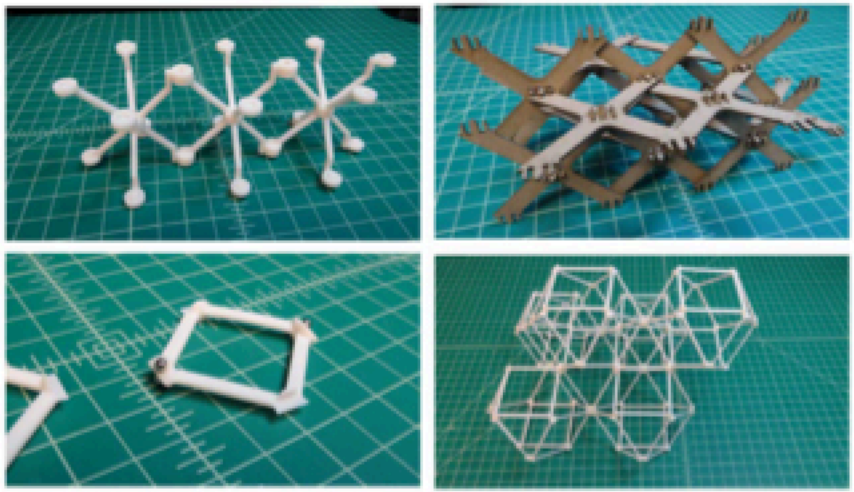

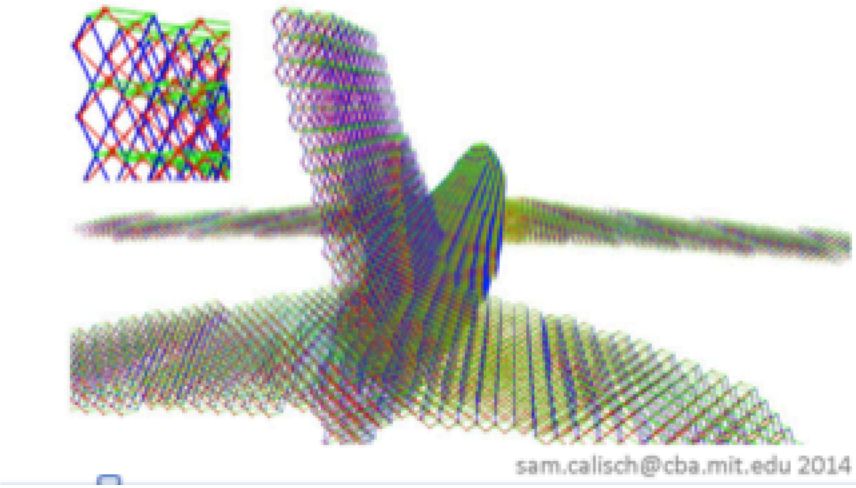

Technical Approach

- **Development of lattice-based digital composite wing structures**
  - Design and fabrication process
  - Bench-testing
  - Preliminary wind tunnel tests at MIT
- **Modeling and control of lattice structures**
  - Physical finite element; lumped mass
  - Discrete-time transfer matrix method
  - Optimal decentralized controls
- **Wind tunnel testing of digital wings**
  - 12-FT low speed tunnel at LaRC
  - Assess aerodynamic characteristics
  - Control authority via wing shaping

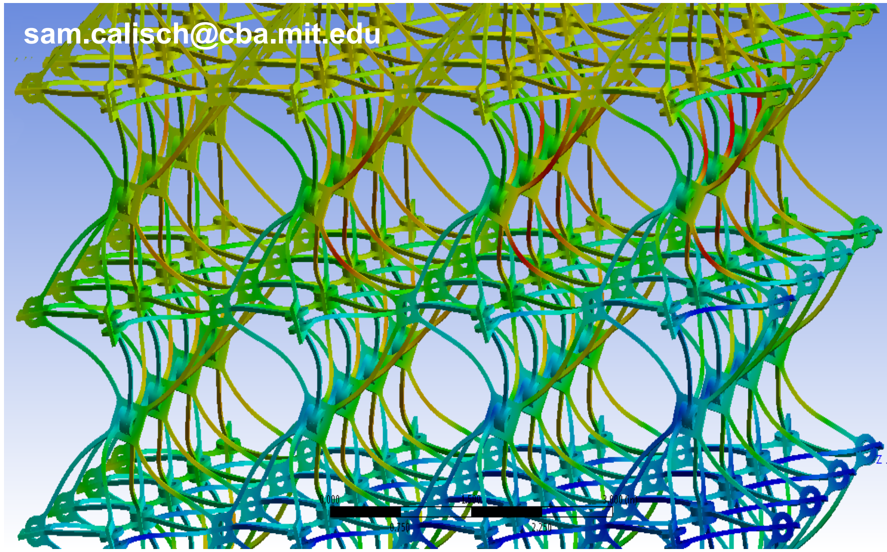

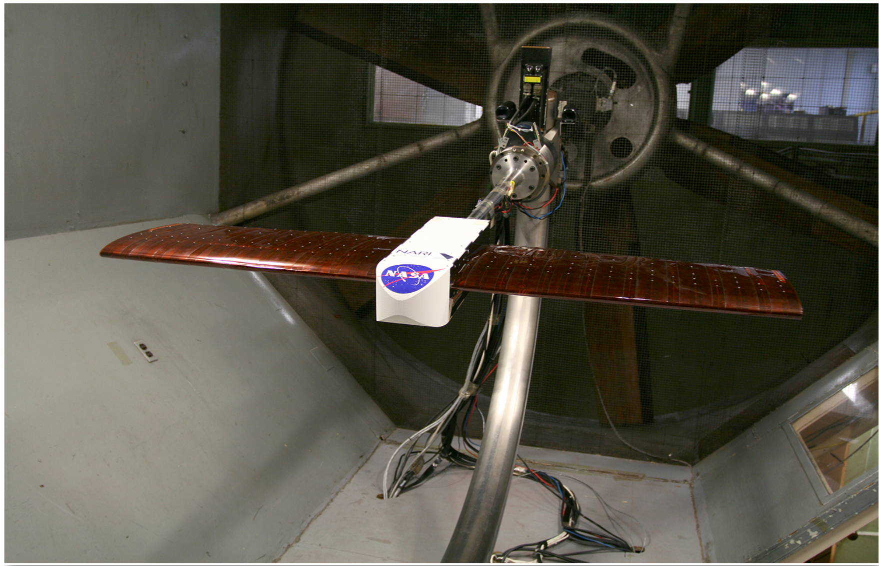

NARI
NASA AERONAUTICS RESEARCH INSTITUTE

Massachusetts Institute of Technology

THE CENTER FOR BITS AND ATOMS

NASA

Development of Lattice-based Digital composite Wing Structures

Team Members

Benjamin Jenett (MIT)
Daniel Cellucci (Cornell)
Nick Cramer (UCSC)
Sam Calisch (CBA, MIT)
Dick Perdichizzi (A&AE, MIT)
Neil Gershenfeld (CBA, MIT)
Robert Nakamura (ARC)
Kenny Cheung (ARC)

Morphing Wings, Lattice Wings

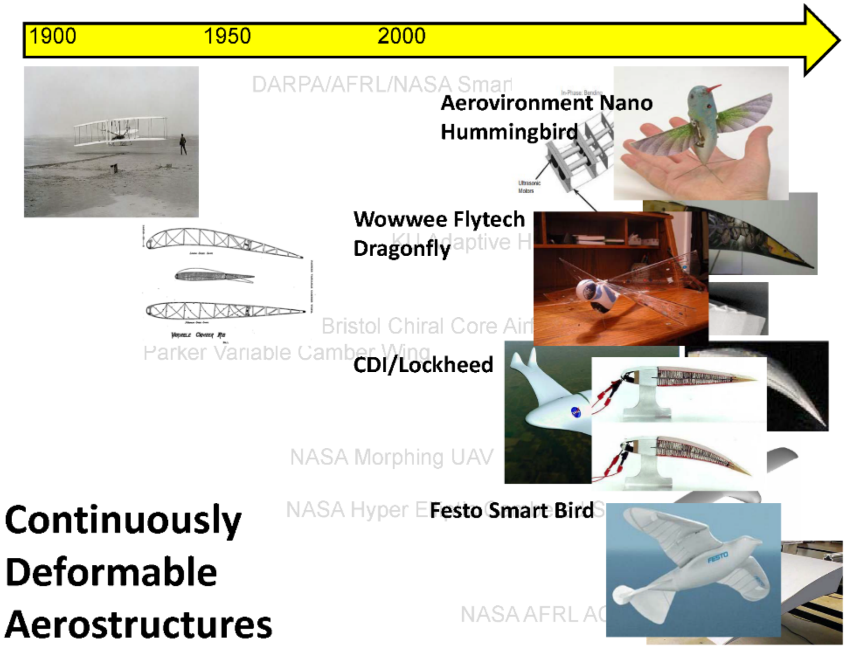

Continuously Deformable Aerostructures

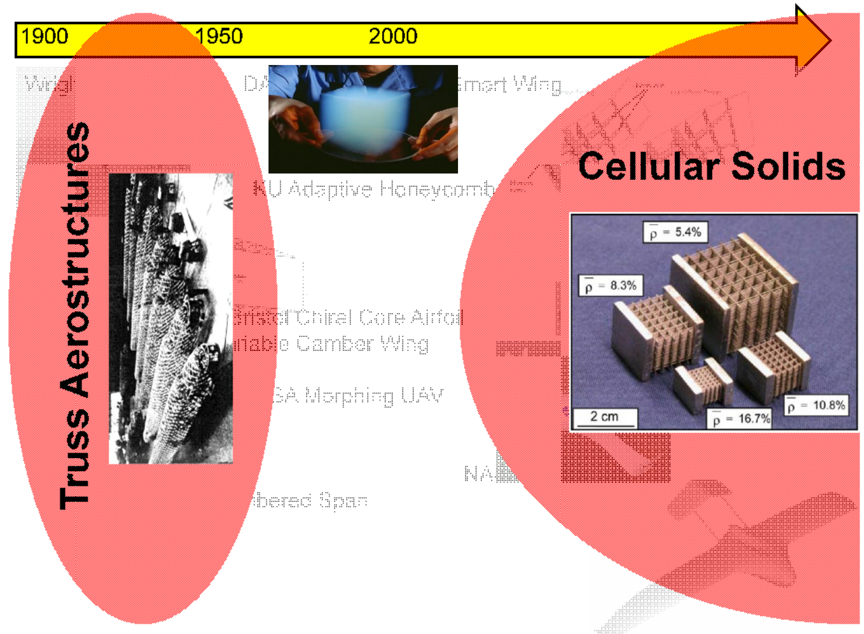

$$\frac{\rho}{\rho_s} = \frac{\rho_c}{\rho_s}(connection\ contribution) + \frac{\rho_l}{\rho_s}(ligament\ contribution)$$

$$\frac{\rho}{\rho_s} = C_c\frac{t^2}{l^2} + C_l\frac{t^2}{l^2} \propto \frac{t^2}{l^2}$$

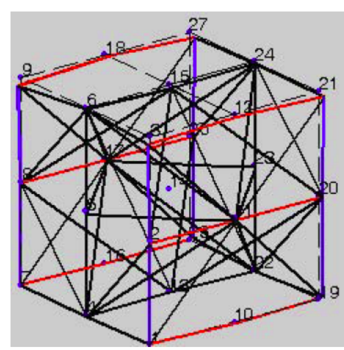

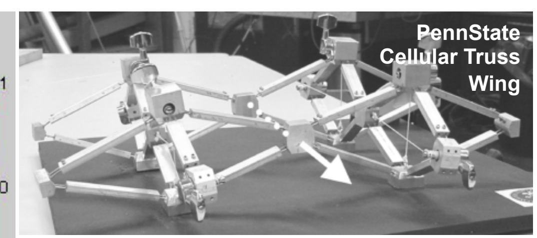

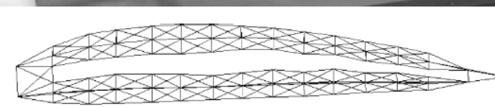

Morphing Lattice Wings

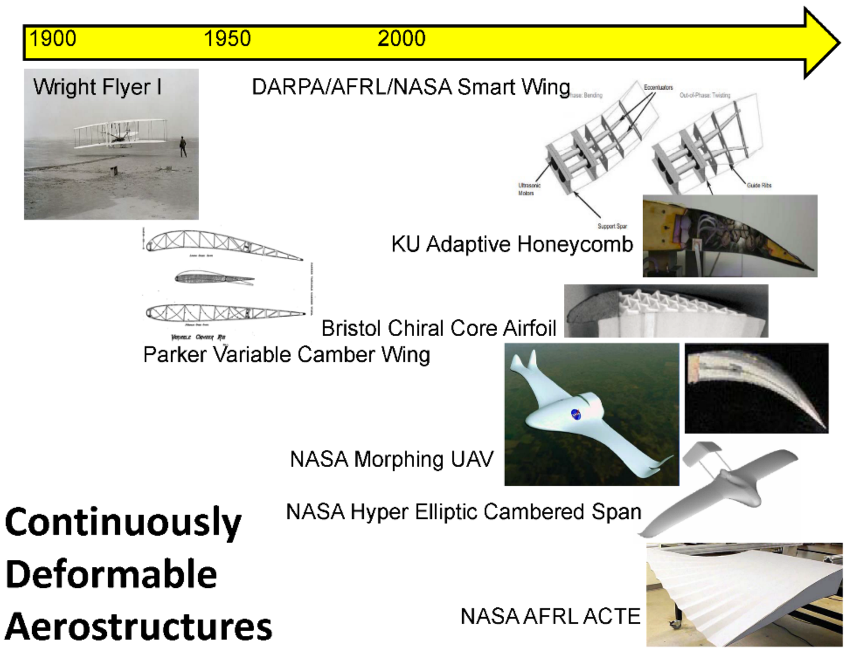

Continuously Deformable Aerostructures

$$E/E_s \propto t^2/l^2 + t^4/l^3 \propto (\rho/\rho_s) + (t^2/l)(\rho/\rho_s) \propto (\rho/\rho_s) + (\rho/\rho_s)^n \propto (\rho/\rho_s)^n$$

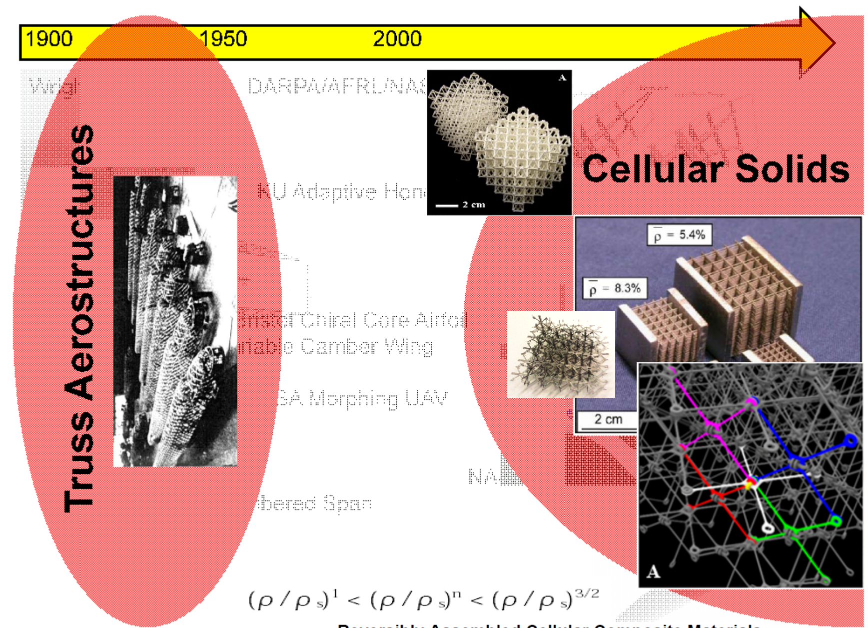

Reversibly Assembled Cellular Composite Materials
Kenneth C. Cheung and Neil Gershenfeld
Science **341**, 1219 (2013);
DOI: 10.1126/science.1240889

$$\delta = \delta_{axial} + \delta_{bending} \propto Fl/E_s t^2 + Fl^2/E_s I \propto Fl^2/E_s I$$

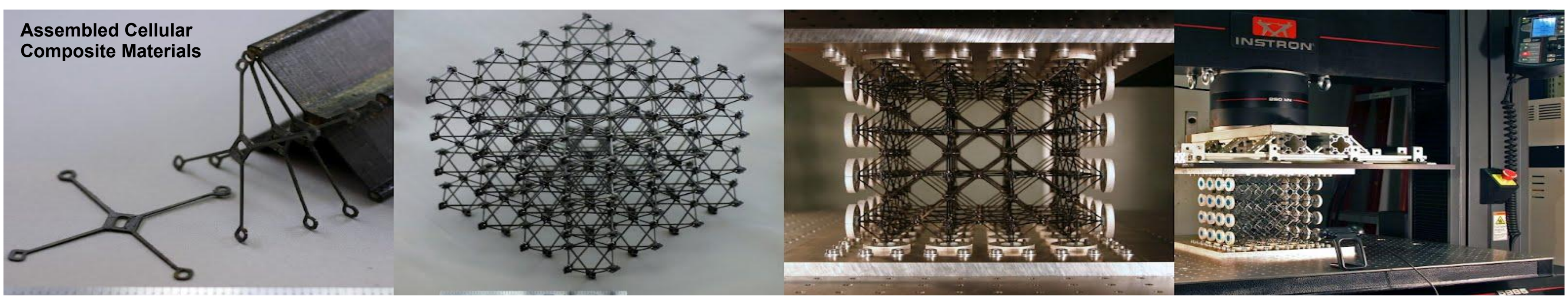

Performance, Flexibility

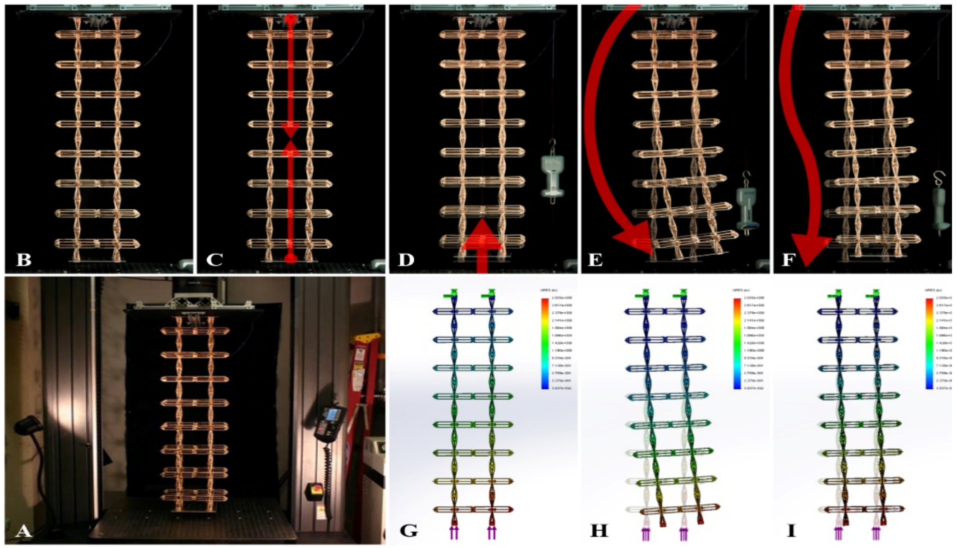

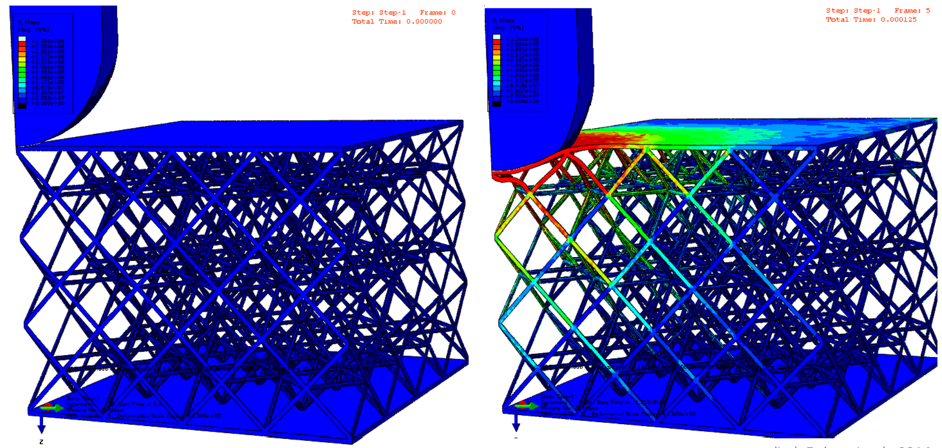

sam.calisch@cba.mit.edu 2014

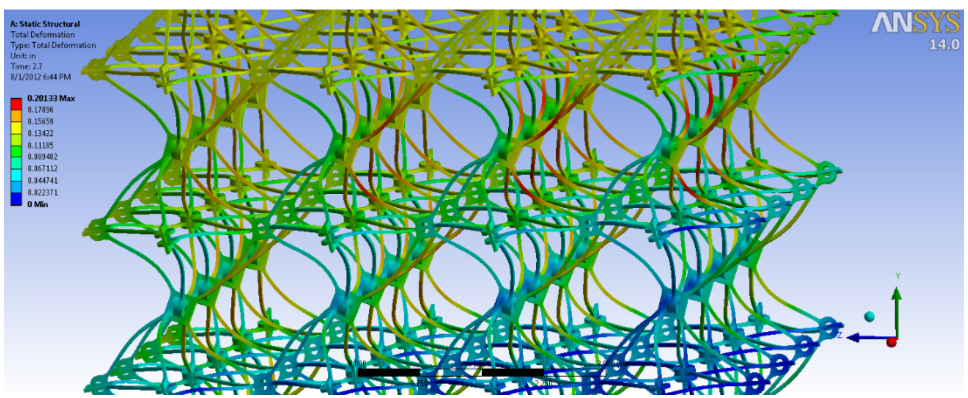

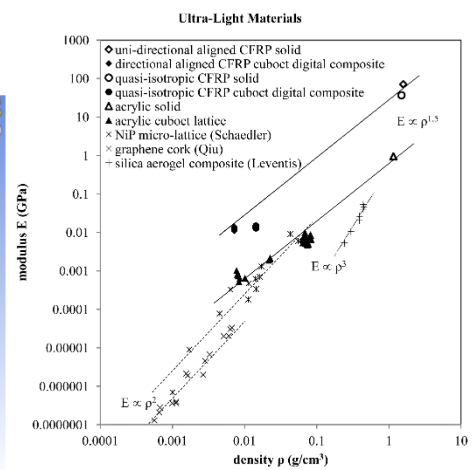

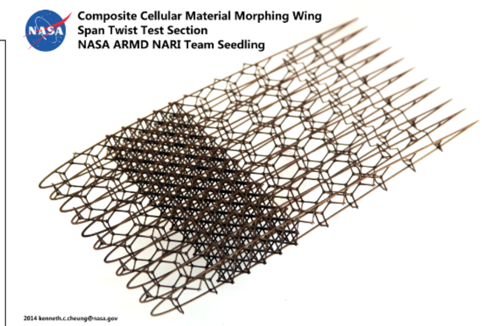

Reversibly Assembled Cellular Composite Materials
Kenneth C. Cheung and Neil Gershenfeld
Science **341**, 1219 (2013);
DOI: 10.1126/science.1240889

2014 kenneth.c.cheung@nasa.gov

NACA0012

- Patch sizing/geometry determination

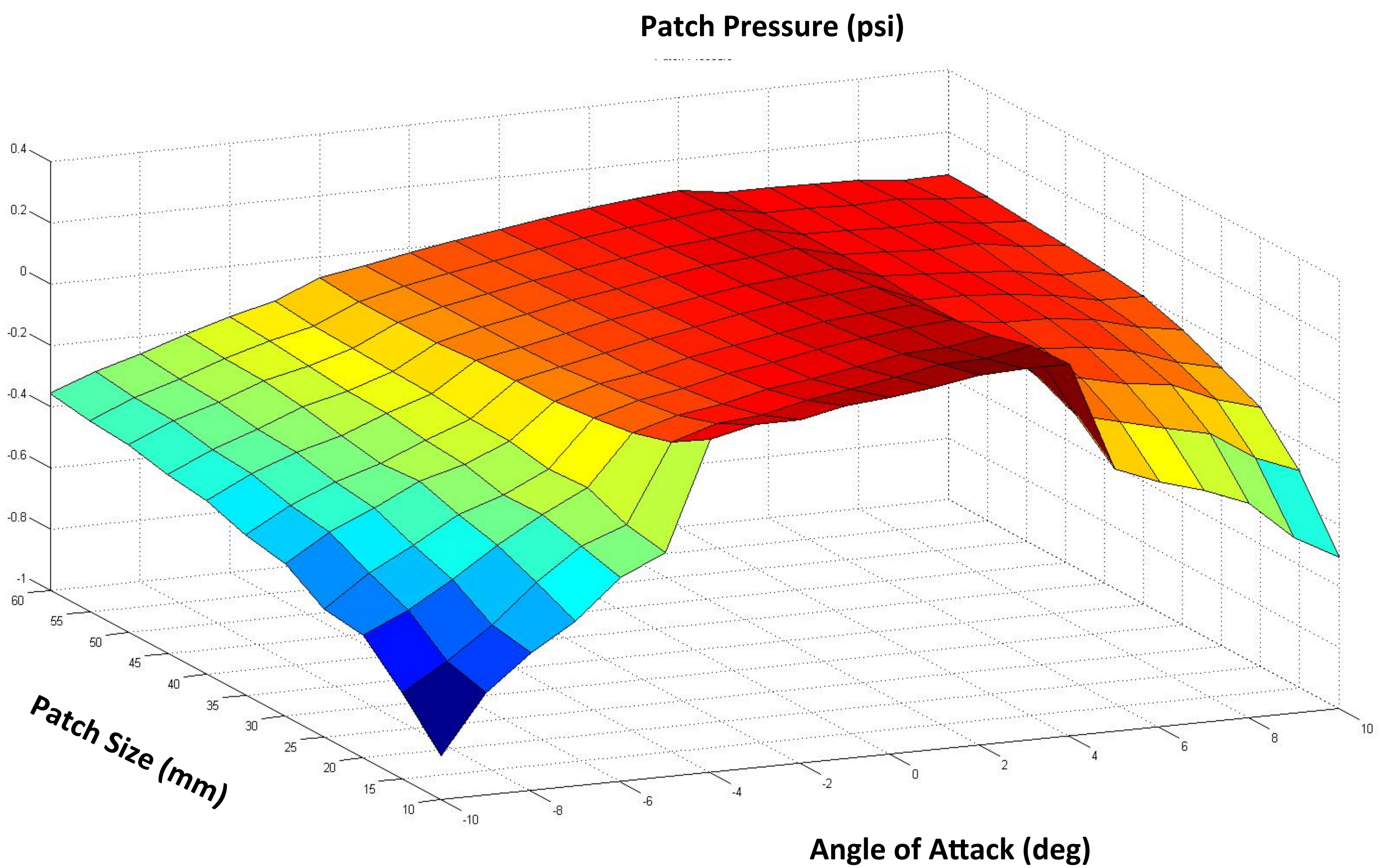

Physical Finite Elements

sam.calisch@cba.mit.edu, MS Thesis, Massachusetts Institute of Technology, 2014

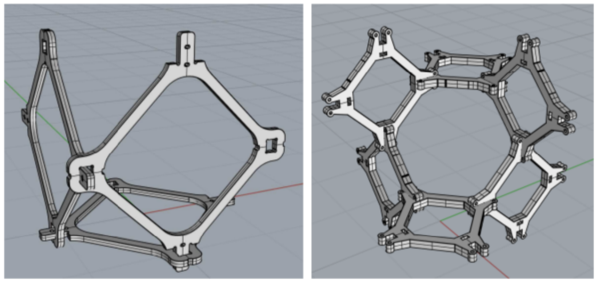

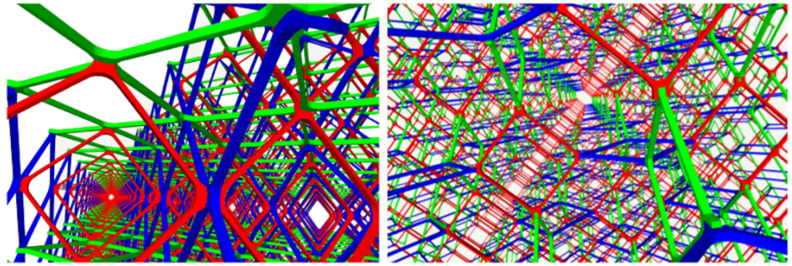

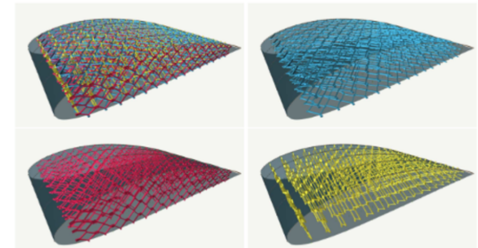

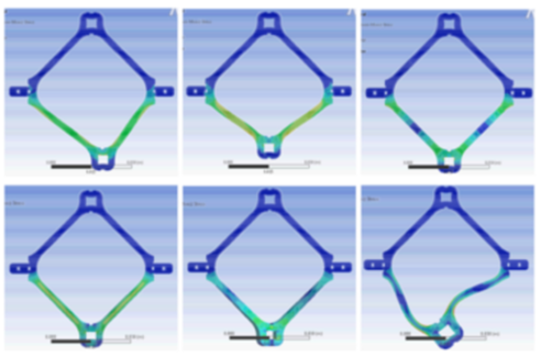

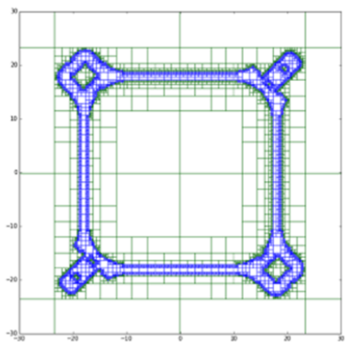

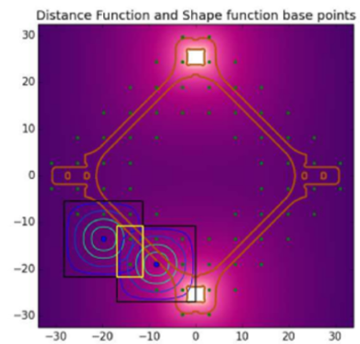

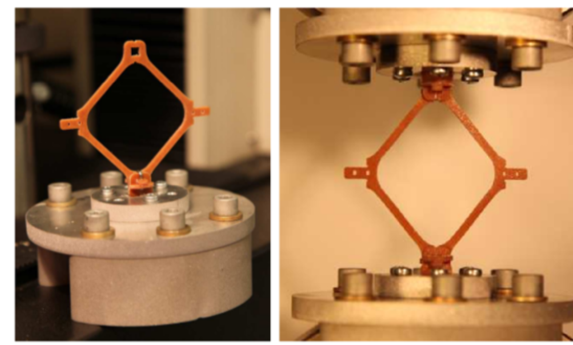

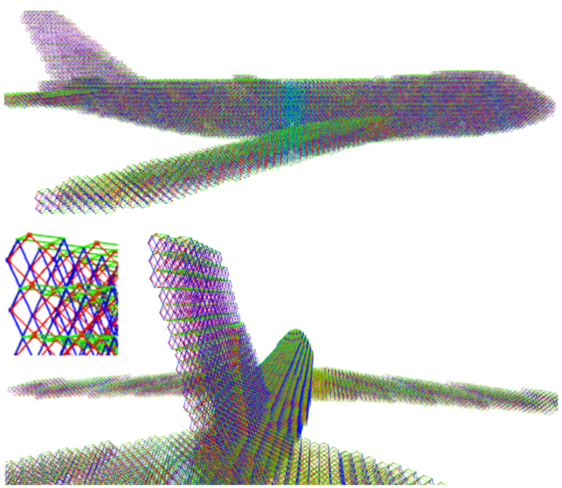

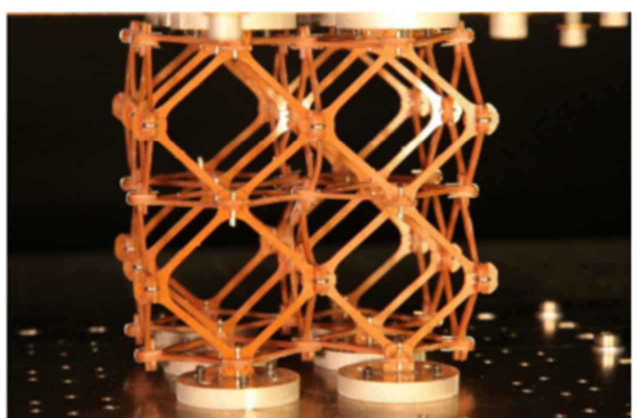

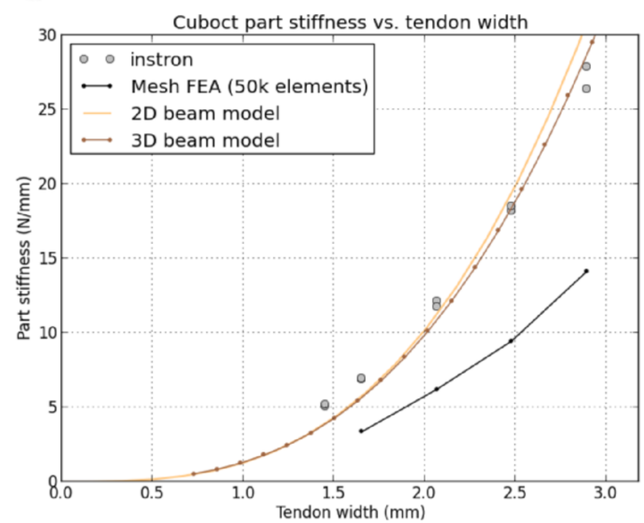

Natural Modes – Simulation

sam.calisch@cba.mit.edu 2014

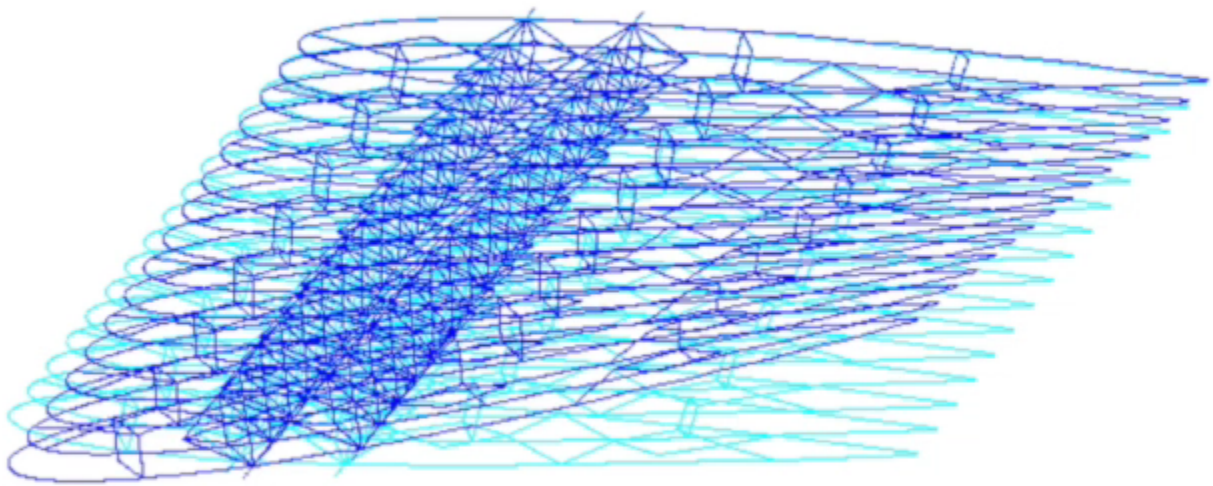

Manufacturing

Boeing 737
~2e6 parts, ~1e6 types, ~24 hour assembly

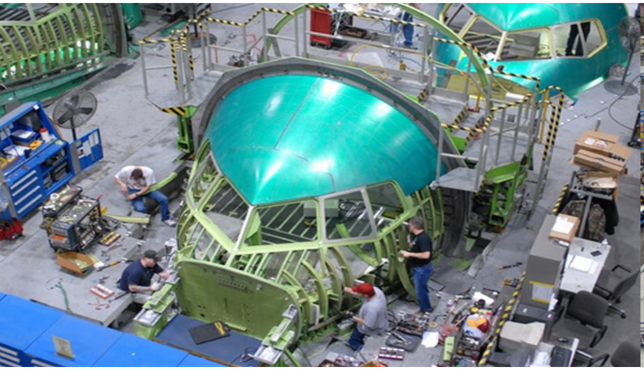

Boeing 787
Goal ~144 hour assembly

(Boeing)

Vickers Wellington, 1935
24 hour production

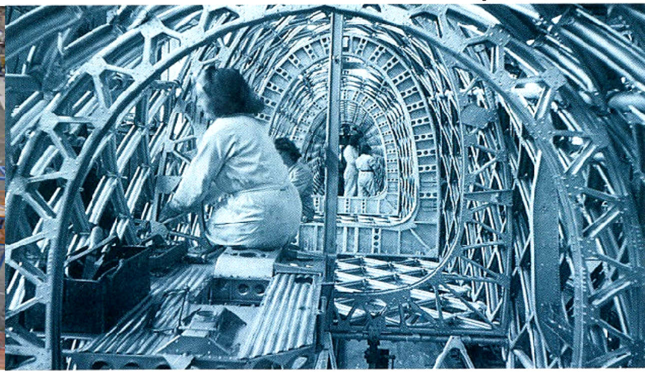

Magnesium metal produced from Harrington sea-water magnesia was vital for wartime production of light alloys used in aircraft frames and for munitions

Wellington Bomber assembly

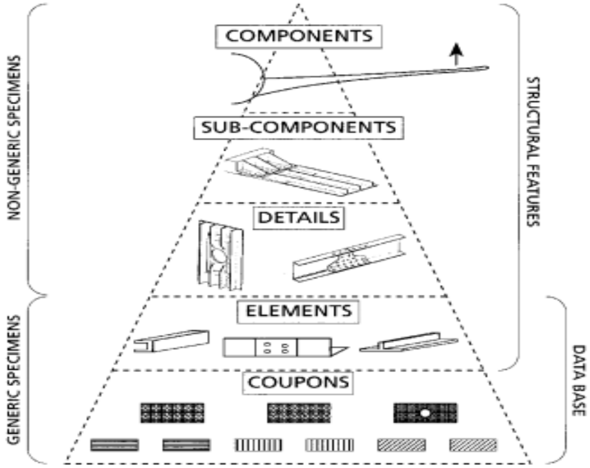

FIGURE 2.1.1 *The pyramid of tests (Reference 2.1.1(a)).*

(Spirit Aerosystems)

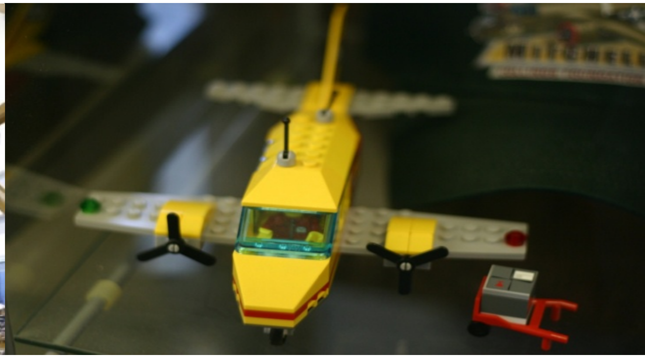

Lego Plane Set # 773x
~200 bricks ~10 types ~100 different planes

Manufacturing

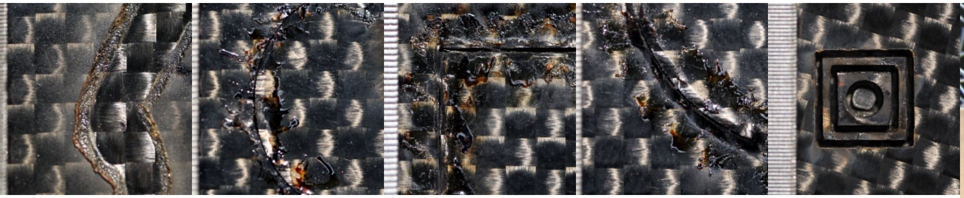

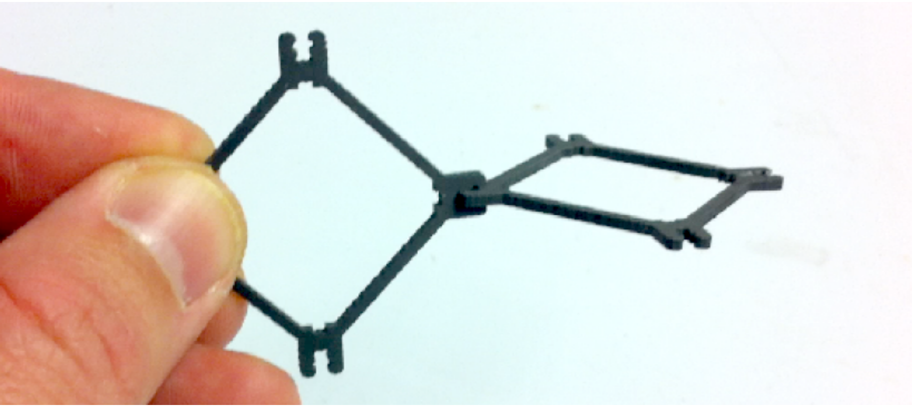

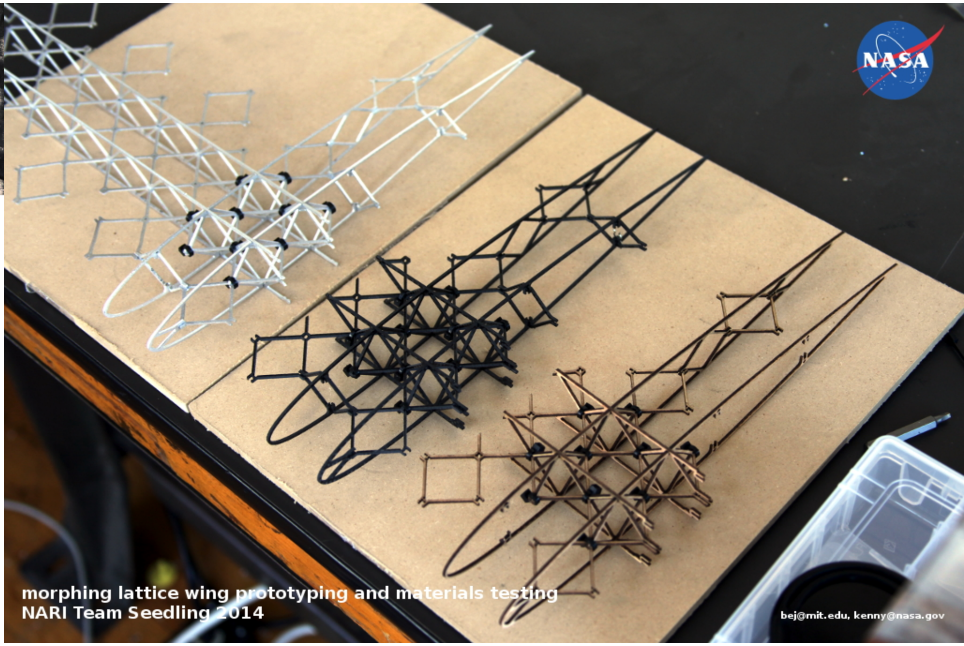

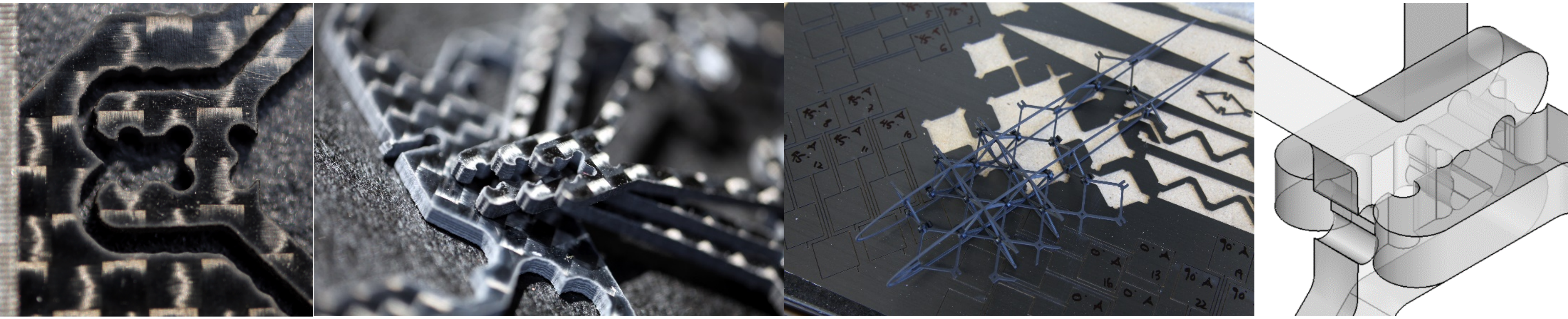

Assembly

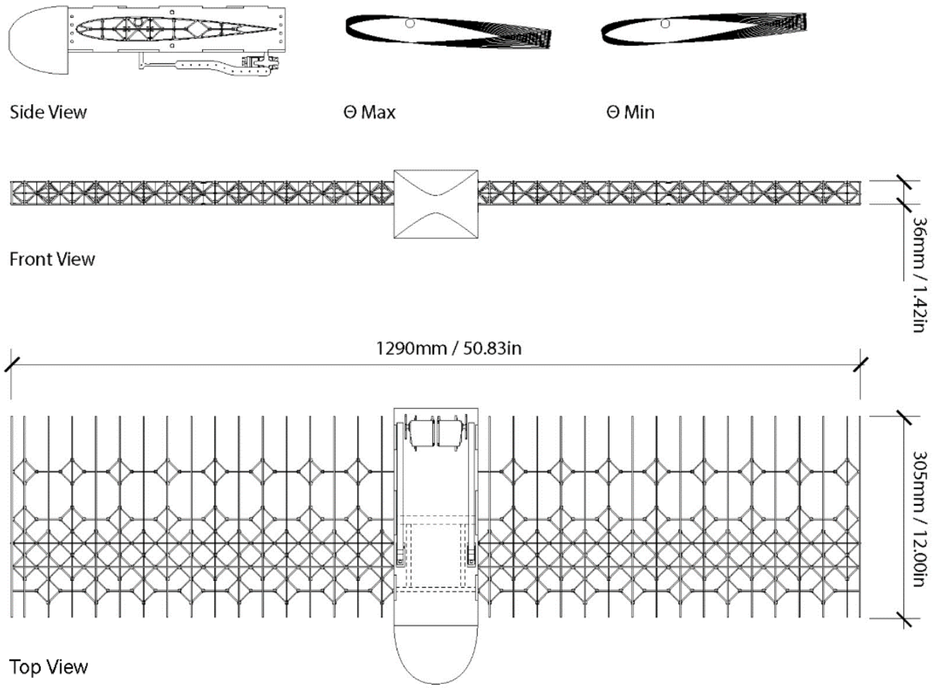

Side View
Θ Max
Θ Min
Front View
36mm / 1.42in
1290mm / 50.83in
305mm / 12.00in
Top View

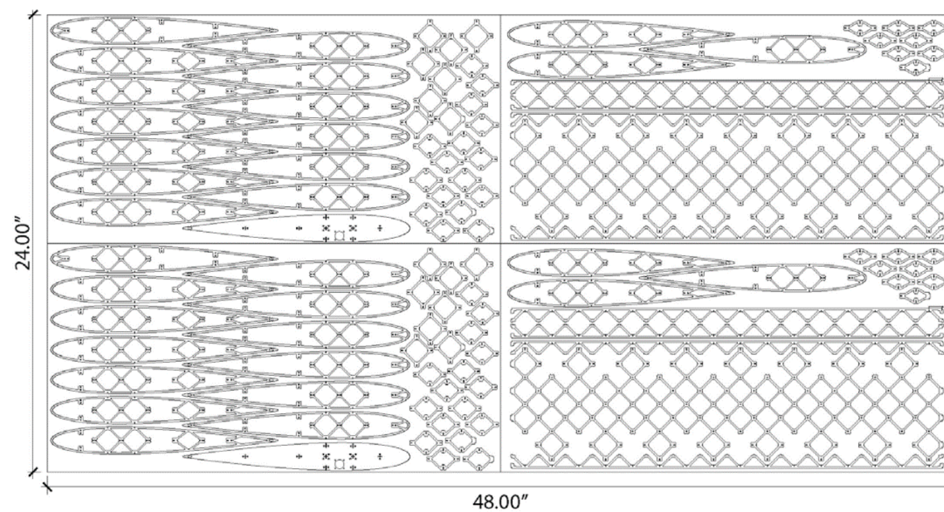

24.00″
48.00″

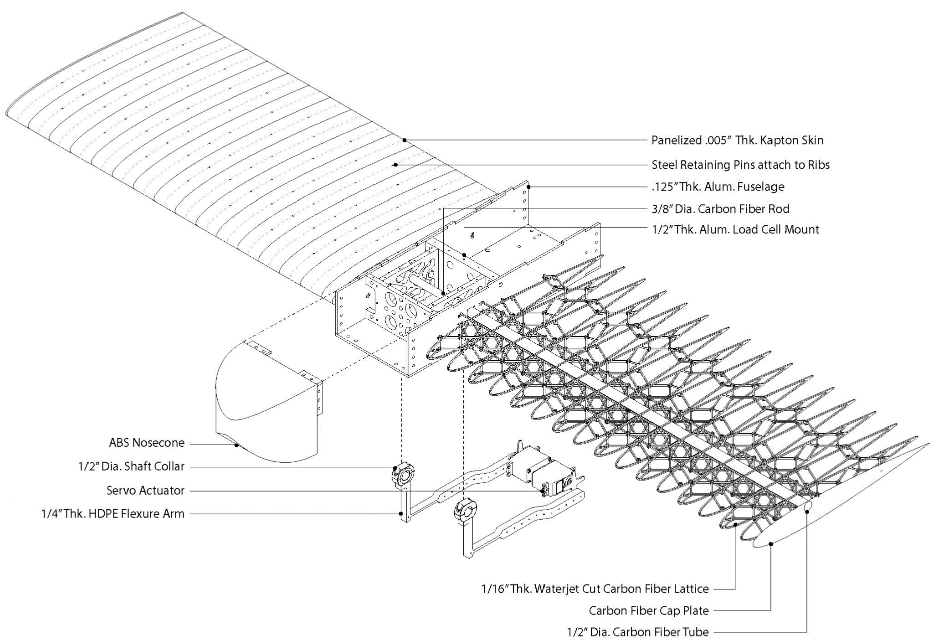

Panelized .005″ Thk. Kapton Skin
Steel Retaining Pins attach to Ribs
.125″Thk. Alum. Fuselage
3/8″Dia. Carbon Fiber Rod
1/2″Thk. Alum. Load Cell Mount
ABS Nosecone
1/2″Dia. Shaft Collar
Servo Actuator
1/4″Thk. HDPE Flexure Arm
1/16″Thk. Waterjet Cut Carbon Fiber Lattice
Carbon Fiber Cap Plate
1/2″ Dia. Carbon Fiber Tube

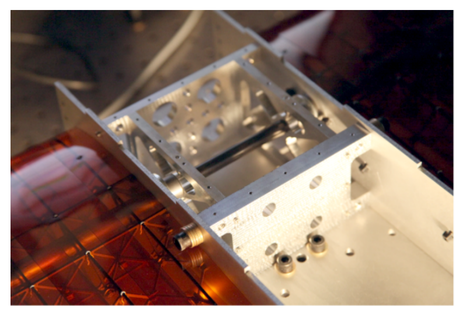

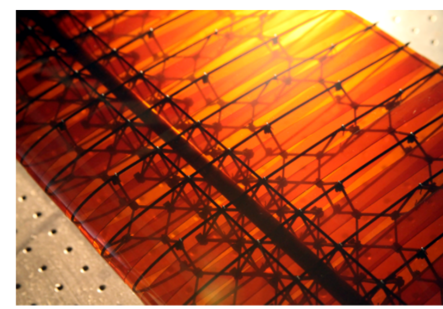

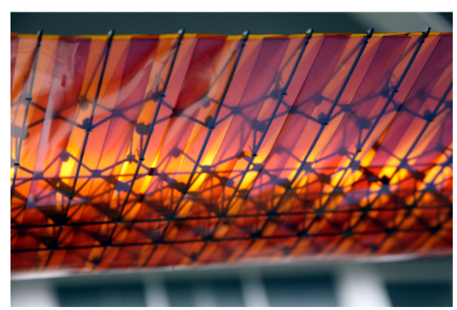

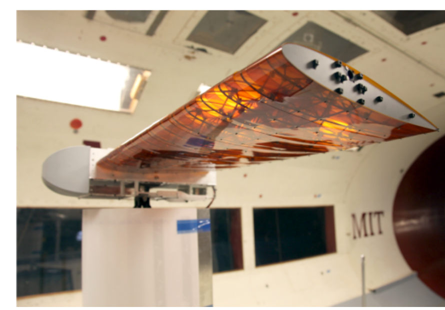

MIT

Bench Testing

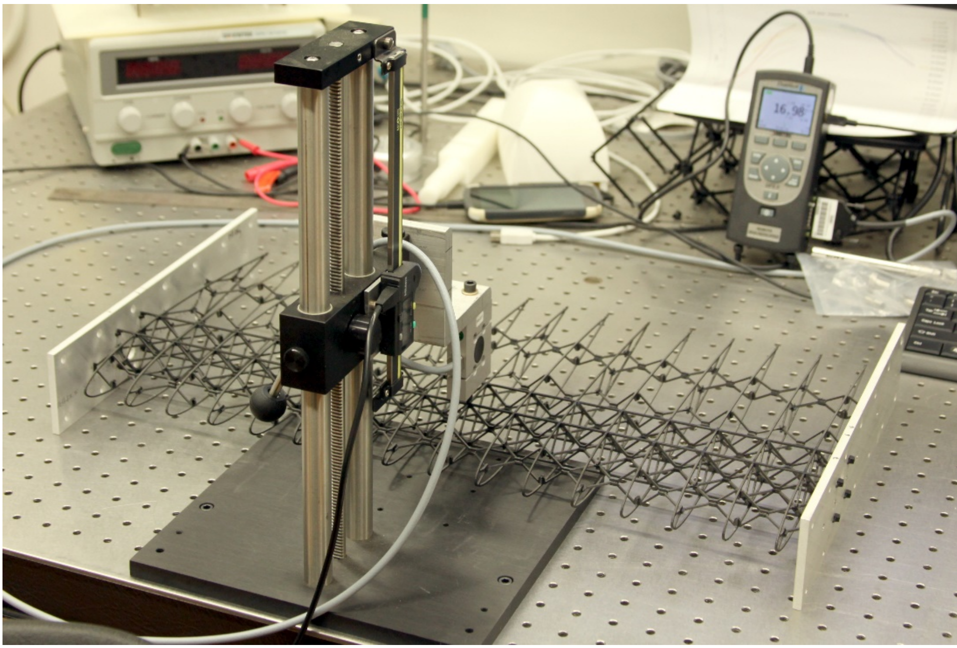

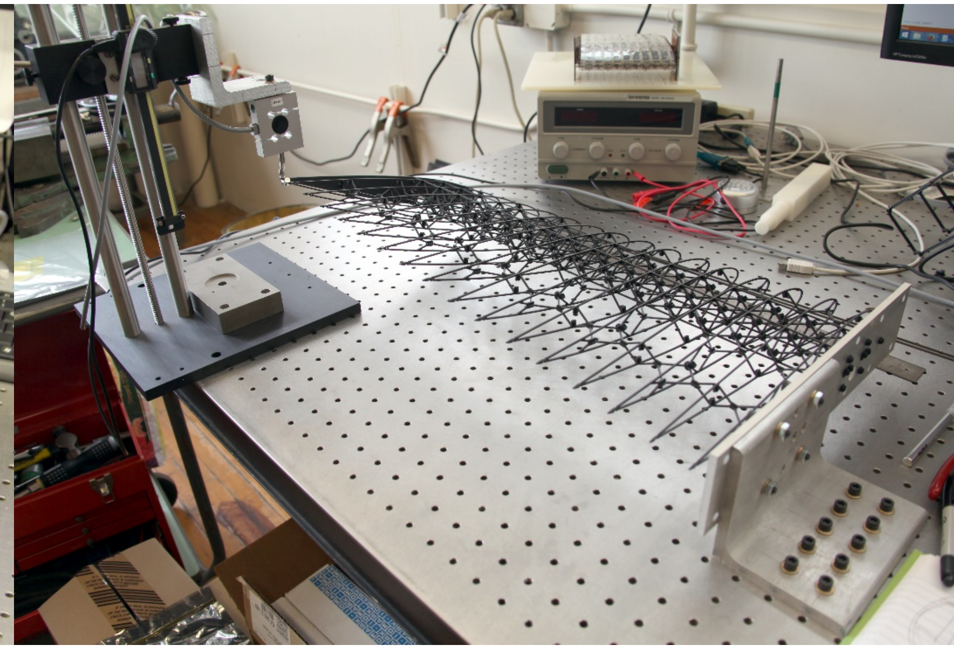

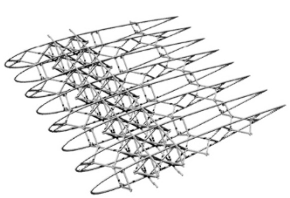

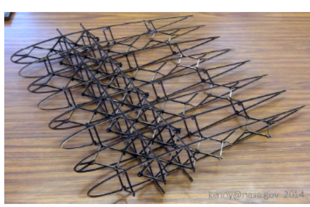

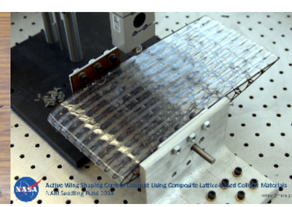

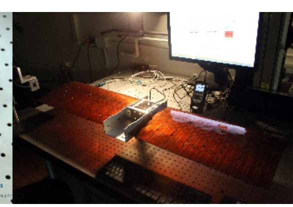

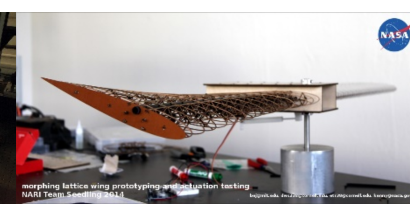

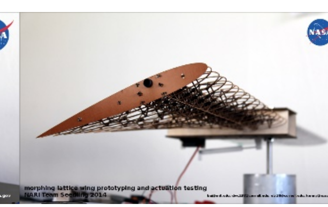

Bench Seat Testing

MIT Wright Brothers 8-ft Tunnel

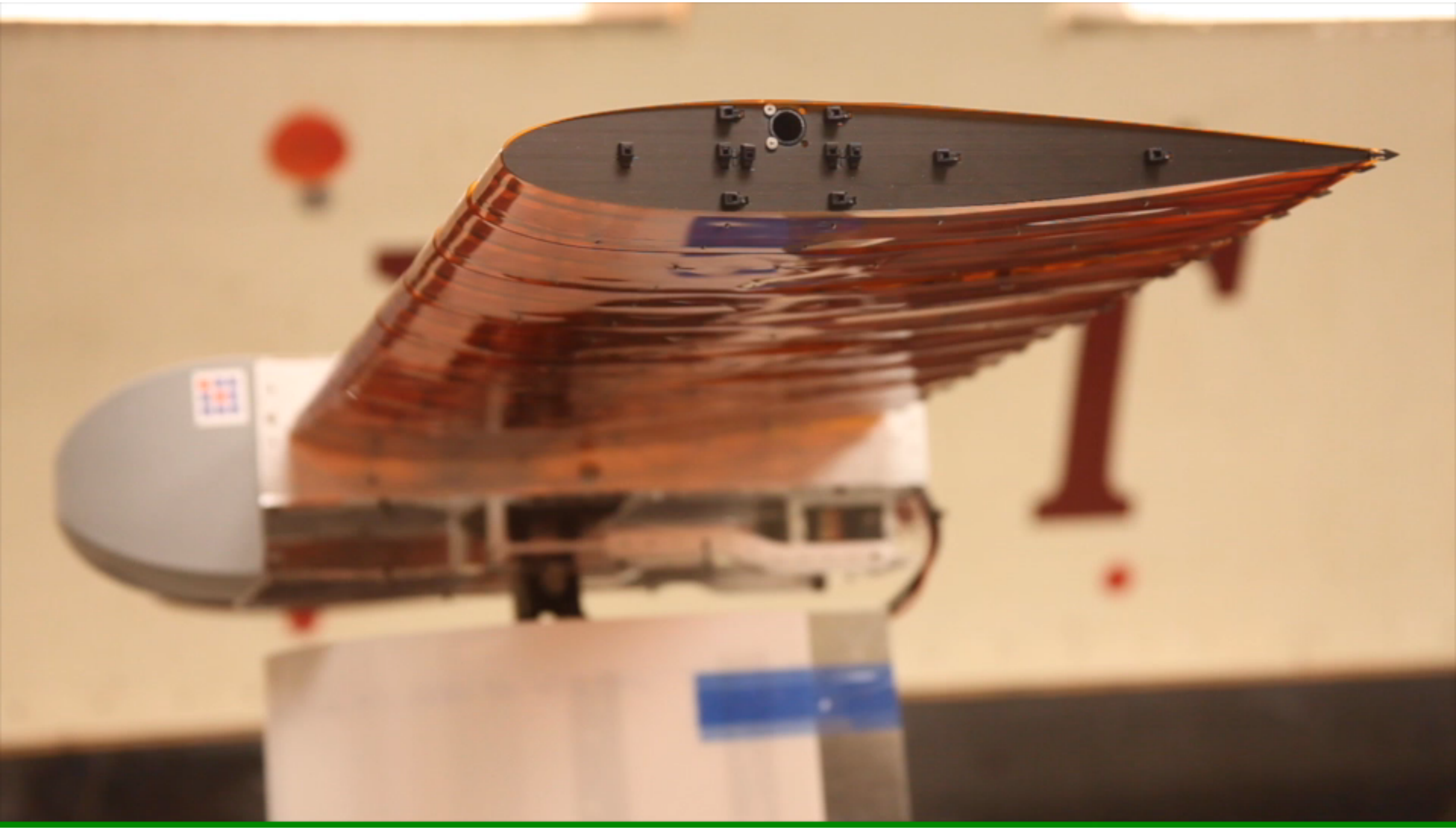

MIT Wright Brothers 8-ft Tunnel

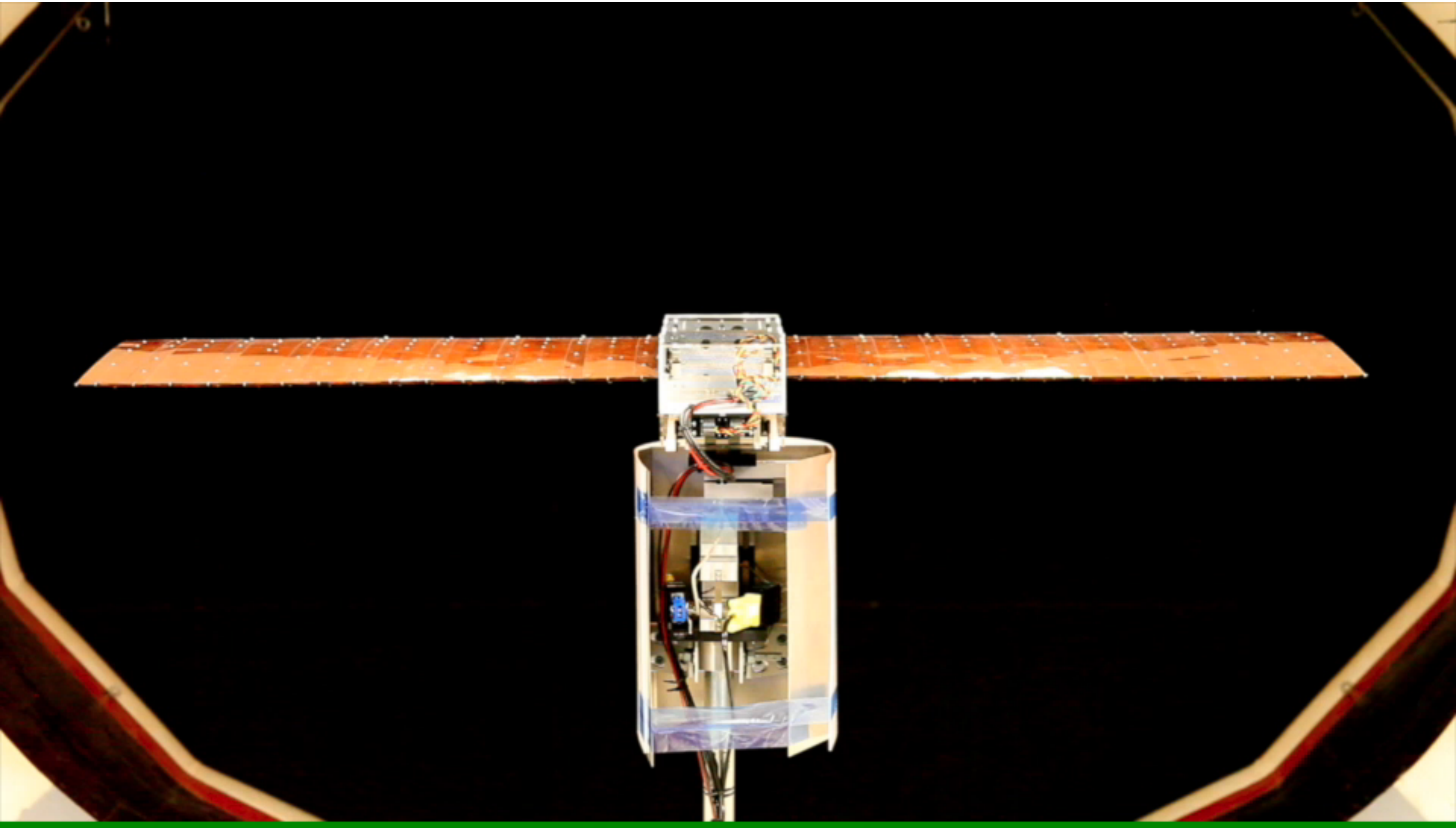

MIT Wright Brothers 8-ft Tunnel

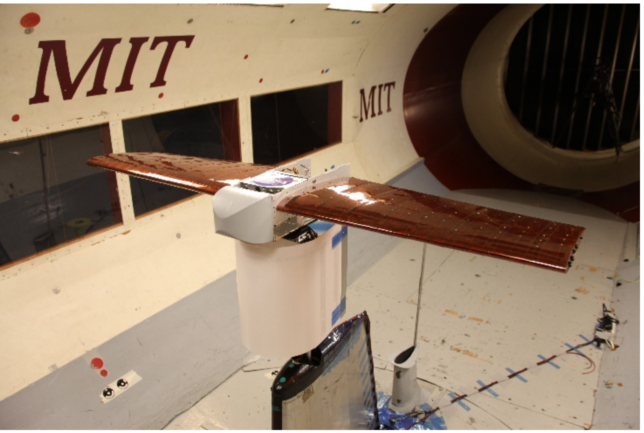

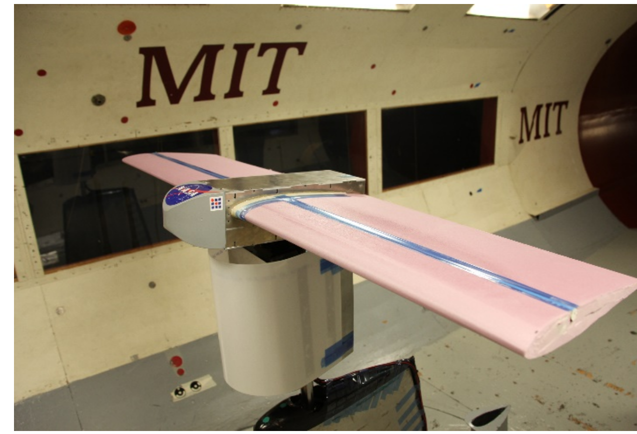

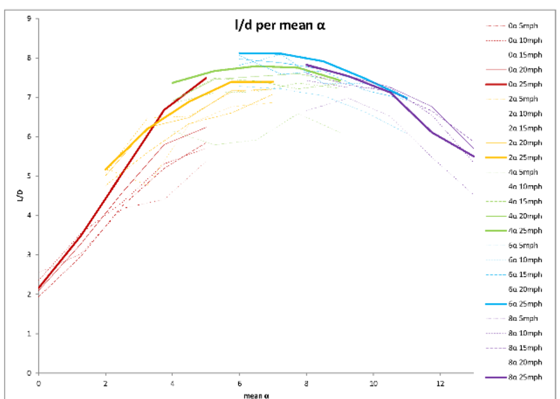

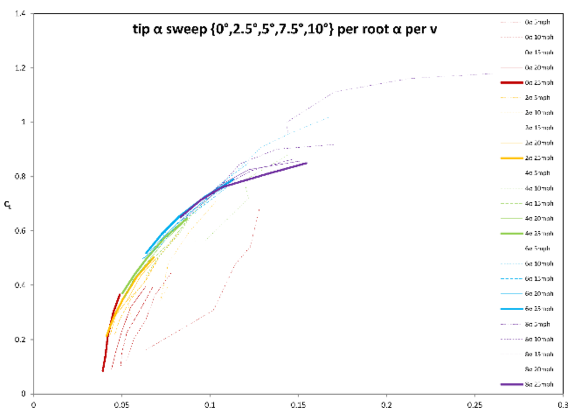

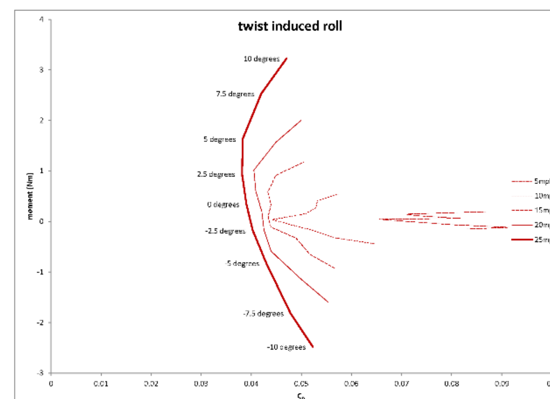

LaRC 12-ft Tunnel

LaRC 12-ft Tunnel

LaRC 12-ft Tunnel

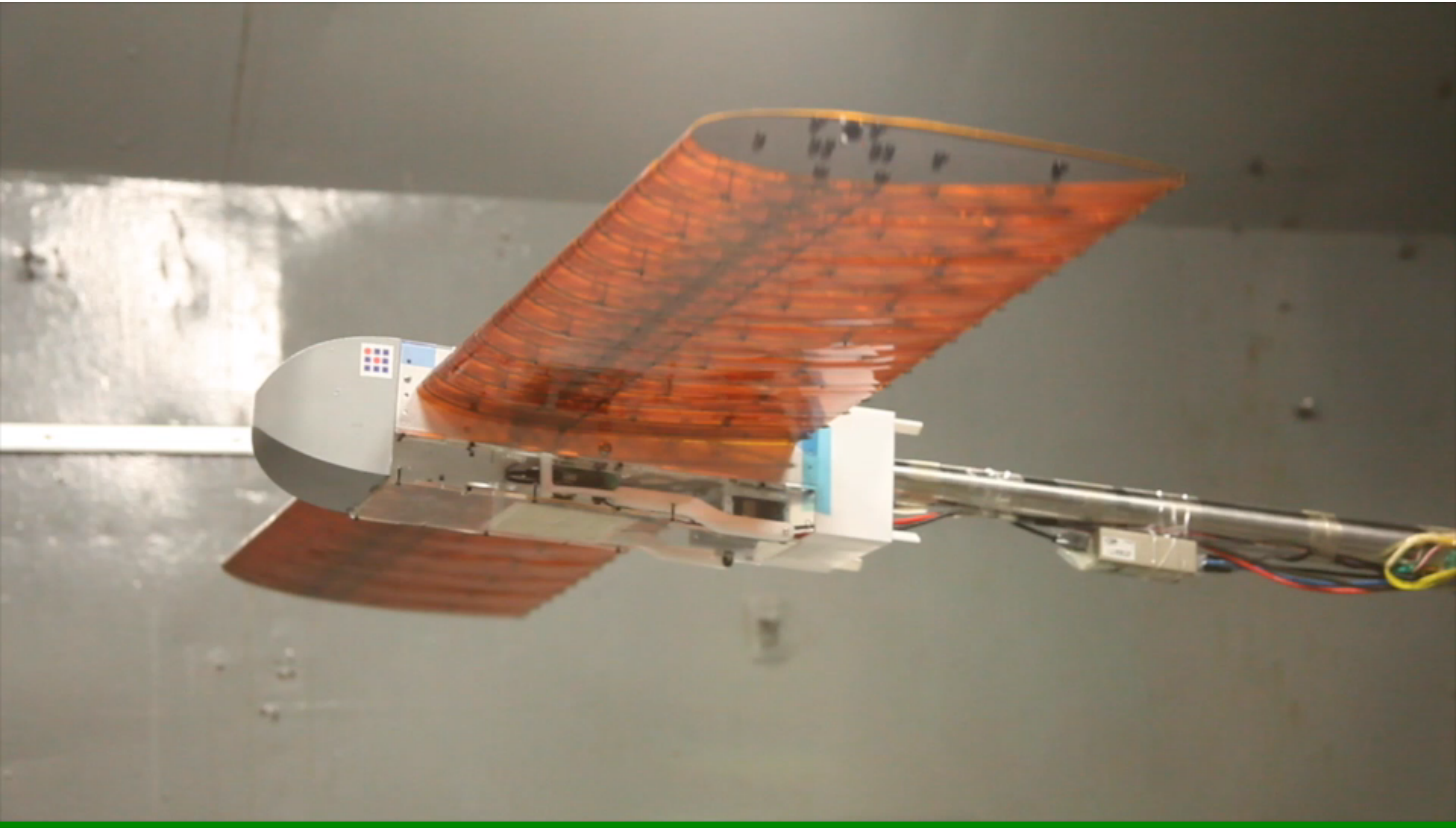

Summary

- Demonstrated successfully the building-block based composite cellular structure concept
- Component level Physical Finite Elements was formulated, analyzed, and validated with test results
- Advanced fabrication and manufacturing process was tested and successfully implemented in producing robust lattice wing structures
- A series of rigorous bench tests and wind tunnel tests were conducted which proved the proposed concept

LaRC 12-ft Test Team – Thanks!

NARI

NASA AERONAUTICS RESEARCH INSTITUTE

NASA

Modeling and Control of Lattice Structures

Team Members

Nick Cramer (UCSC)
Sam Calisch (CBA, MIT)
Neil Gershenfeld (CBA, MIT)
Kenny Cheung (ARC)
Sean Swei (ARC)

Modeling and Control of Lattice Structures

◆ Technical challenges

- Very high dimensions!
- Conventional FEM approach is difficult
- Prone to numerical errors

◆ Development of control-centric model

- Low dimension
- Easy to analyze and simulate
- Suit for control design

◆ Discrete-time Transfer Matrix Method (DT-TMM)

- Suit for interconnected multi-flexible body systems
- Integrating numerical analysis technique with transfer matrix method
- Small matrix operation!

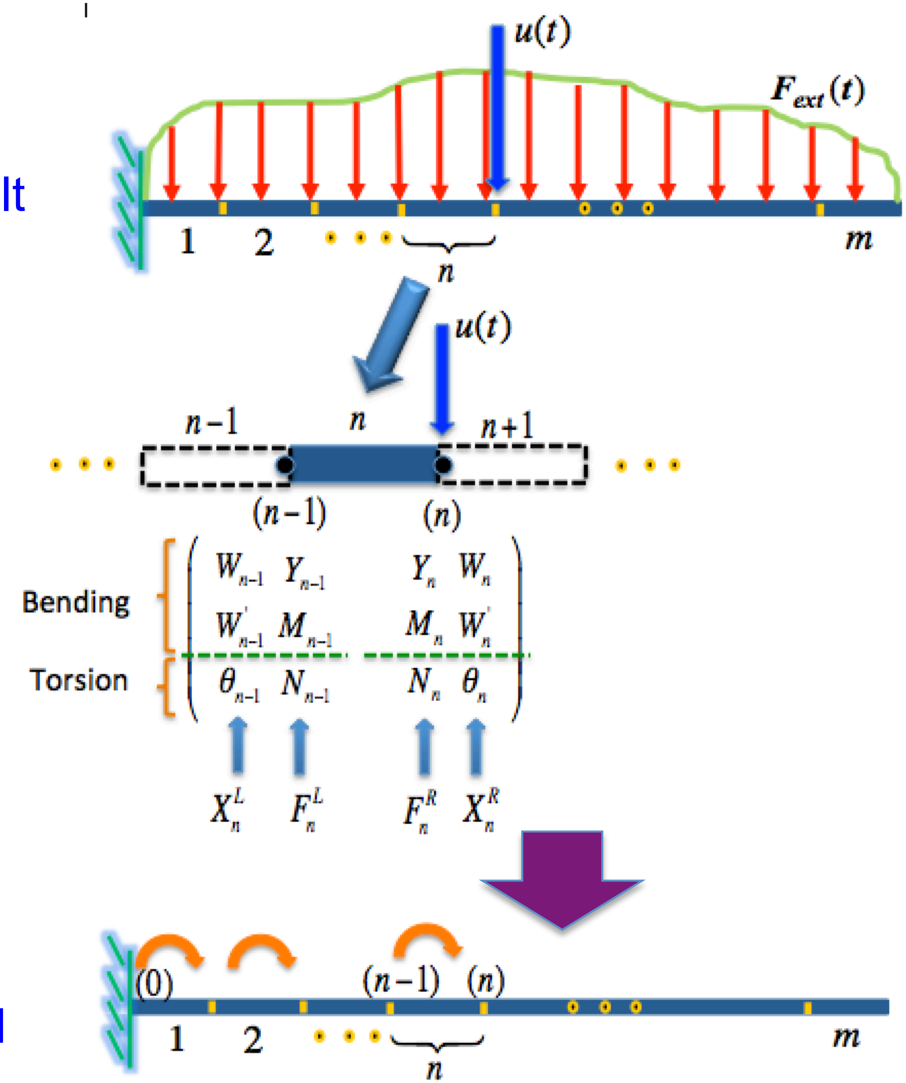

Discrete-time Transfer Matrix Method (DT-TMM)

- Discrete-time lumped mass approximation for cellular structures
  - Easy migration to flight computer
  - Explicit control with maximum bandwidth

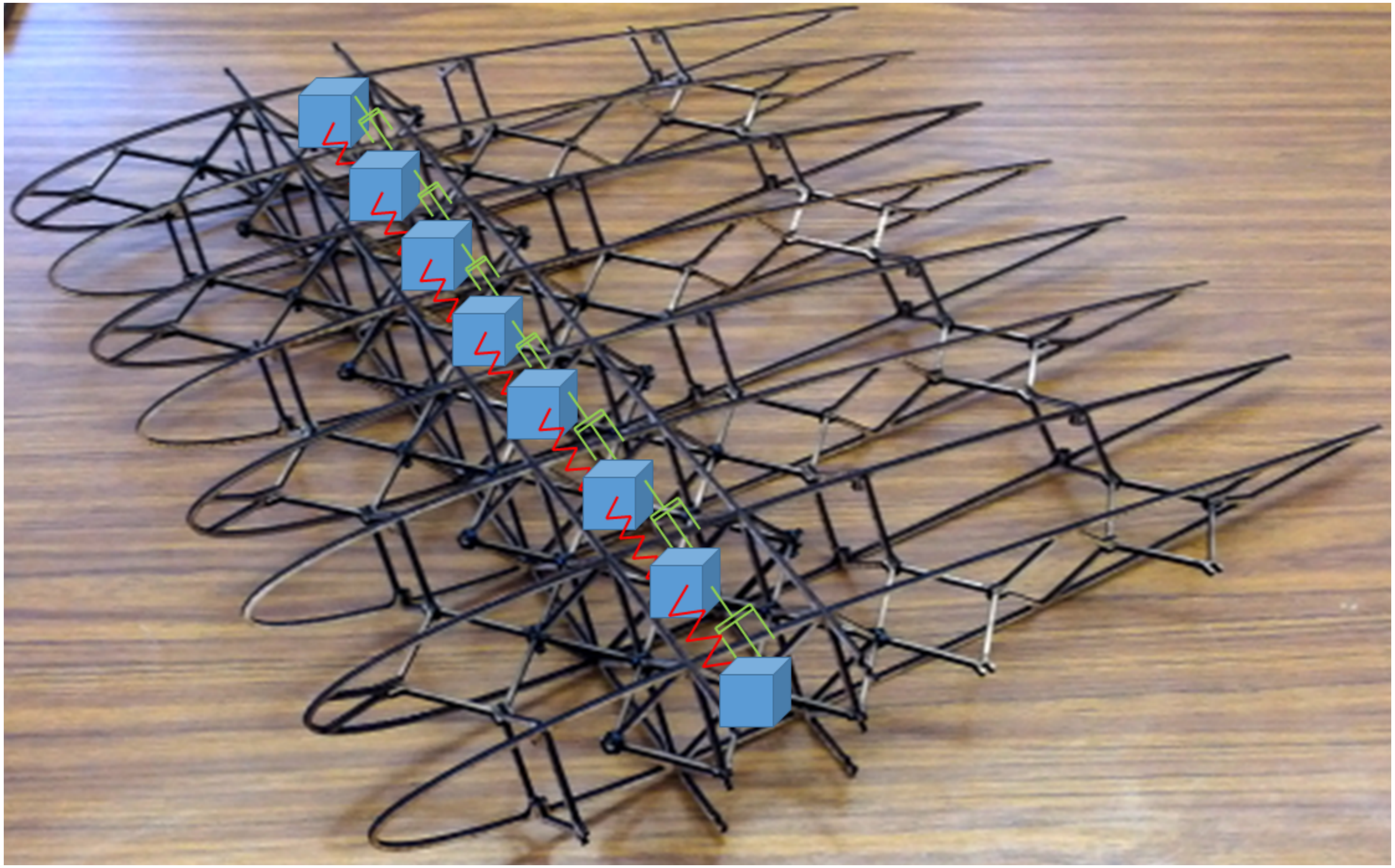

Discrete-time Transfer Matrix Method (DT-TMM)

- Equation of motion for a single element; n^{th}-element

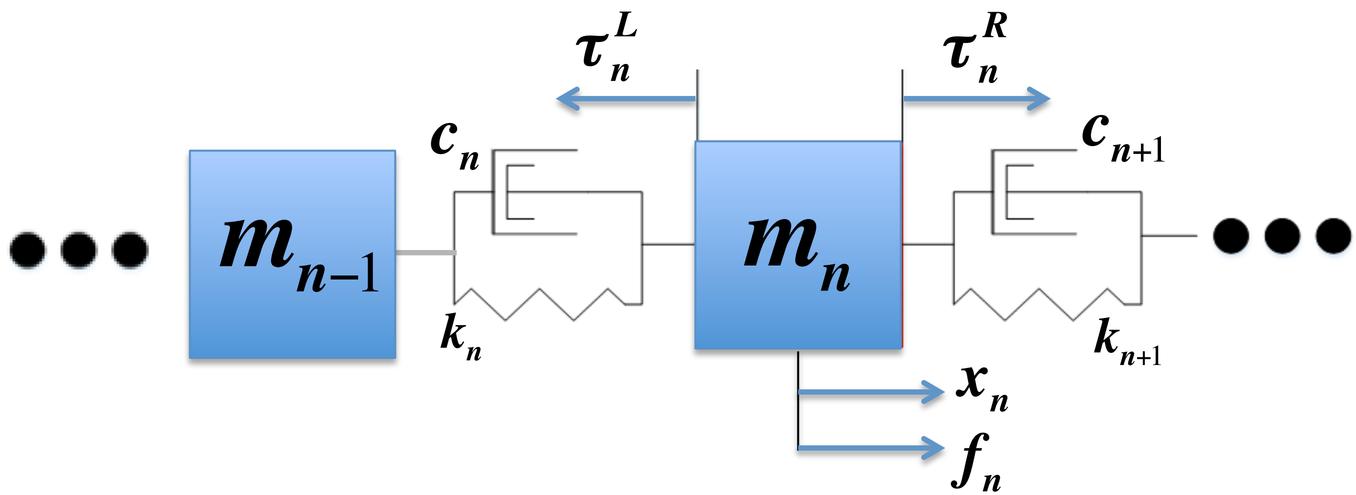

$$m_n \ddot{x}_n(t_i) = \tau_n^R(t_i) - \tau_n^L(t_i) + f_n(t_i)$$

Control input!

where

$$\begin{cases} \tau_n^L(t_i) = k_n(t_i)\left[x_n^L(t_i) - x_{n-1}^R(t_i)\right] + c_n(t_i)\left[\dot{x}_n^L(t_i) - \dot{x}_{n-1}^R(t_i)\right] \\ \tau_n^L = \tau_{n-1}^R \\ x_n^R = x_n^L \end{cases}$$

Discrete-time Transfer Matrix Method (DT-TMM)

- General Discretization; n^{th}-element

$$\begin{cases} \ddot{x}_n(t_i) = A_n(t_i)x_n(t_i) + B_n(t_i) \\ \dot{x}_n(t_i) = D_n(t_i)x_n(t_i) + E_n(t_i) \end{cases}$$

Therefore, we obtain

$$m_n(A_n x_n + B_n) = \tau_n^R - \tau_n^L + f_n$$

and

$$\tau_n^L = k_n\left[x_n^L - x_{n-1}^R\right] + c_n\left[\left(D_n x_n + E_n\right)^L - \left(D_{n-1}x_{n-1} + E_{n-1}\right)^R\right]$$

Note: The quantities A_n, B_n, D_n, and E_n depend on the type of numerical integration scheme used in the analysis!

Discrete-time Transfer Matrix Method (DT-TMM)

- Matrix formulation: From ***LEFT*** to n^{th}-element

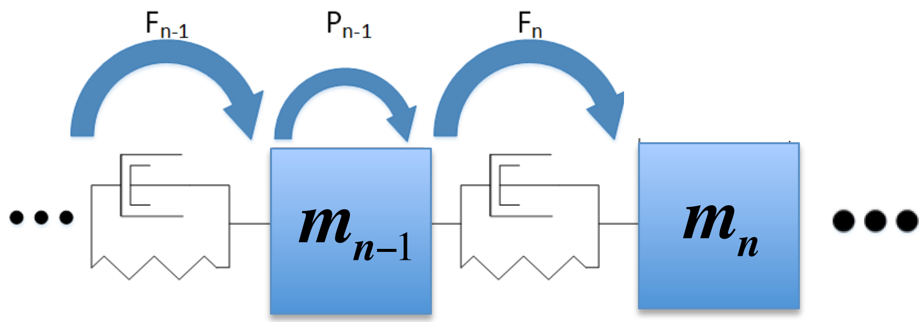

Mass

$$\begin{Bmatrix} x \\ \tau \\ 1 \end{Bmatrix}_n^R = \begin{bmatrix} 1 & 0 & 0 \\ m_n A_n & 1 & m_n B_n - f_n \\ 0 & 0 & 1 \end{bmatrix} \begin{Bmatrix} x \\ \tau \\ 1 \end{Bmatrix}_n^L \quad \Rightarrow \quad \boldsymbol{v}_n^R = \boldsymbol{P}_n \boldsymbol{v}_n^L$$

Spring-Damper

$$\begin{Bmatrix} x \\ \tau \\ 1 \end{Bmatrix}_n^L = \begin{bmatrix} \frac{k_n + c_n D_{n-1}^R}{k_n + c_n D_n^L} & \frac{1}{k_n + c_n D_n^L} & \frac{-c_n (E_n^L - E_{n-1}^R)}{k_n + c_n D_n^L} \\ 0 & 1 & 0 \\ 0 & 0 & 1 \end{bmatrix} \begin{Bmatrix} x \\ \tau \\ 1 \end{Bmatrix}_{n-1}^R \quad \Rightarrow \quad \boldsymbol{v}_n^L = \boldsymbol{F}_n \boldsymbol{v}_{n-1}^R$$

Discrete-time Transfer Matrix Method (DT-TMM)

- Matrix formulation: From ***RIGHT*** to n^{th}-element

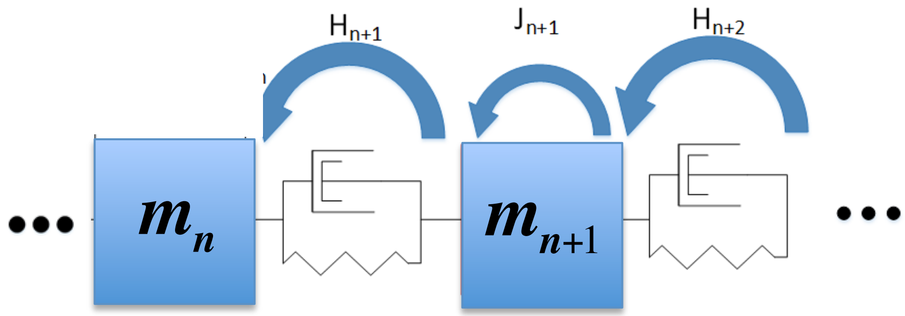

Mass

$$\begin{Bmatrix} x \\ \tau \\ 1 \end{Bmatrix}_n^L = \begin{bmatrix} 1 & 0 & 0 \\ -m_n A_n & 1 & -m_n B_n + f_n \\ 0 & 0 & 1 \end{bmatrix} \begin{Bmatrix} x \\ \tau \\ 1 \end{Bmatrix}_n^R$$

$\Rightarrow$ $v_n^L = J_n v_n^R$

Spring-Damper

$$\begin{Bmatrix} x \\ \tau \\ 1 \end{Bmatrix}_n^R = \begin{bmatrix} \frac{k_n + c_n D_{n-1}^R}{k_n + c_n D_n^L} & \frac{1}{k_n + c_n D_n^L} & \frac{-c_n (E_n^L - E_{n+1}^R)}{k_n + c_n D_n^L} \\ 0 & 1 & 0 \\ 0 & 0 & 1 \end{bmatrix} \begin{Bmatrix} x \\ \tau \\ 1 \end{Bmatrix}_{n+1}^L$$

$\Rightarrow$ $v_n^R = H_n v_{n+1}^L$

Discrete-time Transfer Matrix Method (DT-TMM)

- Propagation from ***BOTH*** sides to n^{th}-element

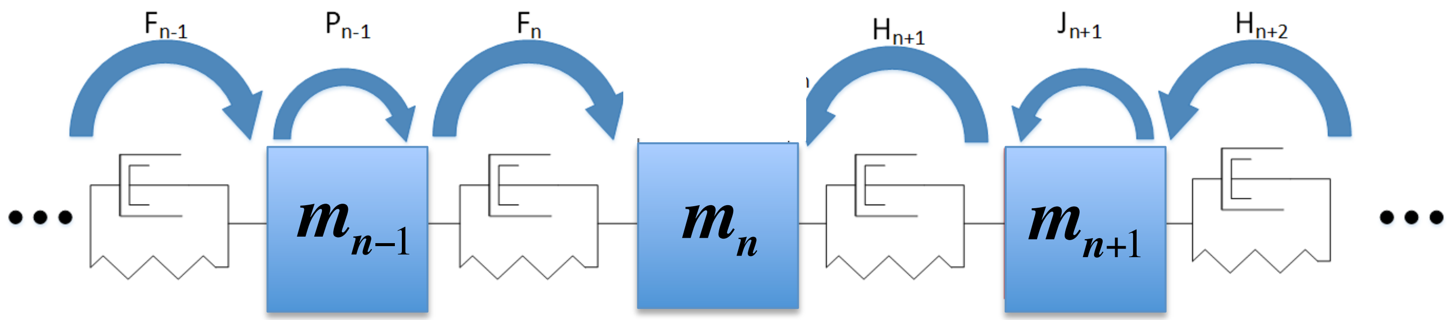

Left to right propagation: $Q_n = \prod_{i=0}^{n} P_i F_i$

Right to left propagation: $T_n = \prod_{i=m}^{n} H_i J_i$

Combination of Q and T:
$$\begin{cases} v_n^L = F_n Q_n v_0^R \\ v_n^R = T_n v_m^R \\ m_n(A_n x_n + B_n) = \tau_n^R - \tau_n^L + f_n \end{cases}$$

Full system description in terms of LOCAL degree of freedom; n^{th}-element

Discrete-time Transfer Matrix Method (DT-TMM)

- Third order Houbolt numerical integration method was chosen
- Decentralized control problem formulation:

$$x_n(t_i) = Ax_n(t_{i-1}) + B(\alpha + f_n)^{**}$$

Linear discrete-time system!

where α denotes the coupling between nth-element and its neighbors.

- A "weak" coupling can be ensured by making the time step size small; diagonal dominance!
- The control problem can be solved using standard LQR approach:

$$\min_{f_n} J = \sum_{k=0}^{N} x_k^T Q x_k + (f_n)_k^T R (f_n)_k \;\; ; \;\; Q > 0,\; R > 0.$$

**: Cramer et al. "Application of Transfer Matrix Approach to Modeling and Decentralized Control of Lattice-based Structures," appeared in 2015 SciTech Conf.

Discrete-time Transfer Matrix Method (DT-TMM)

- Example: 3-Mass System Control

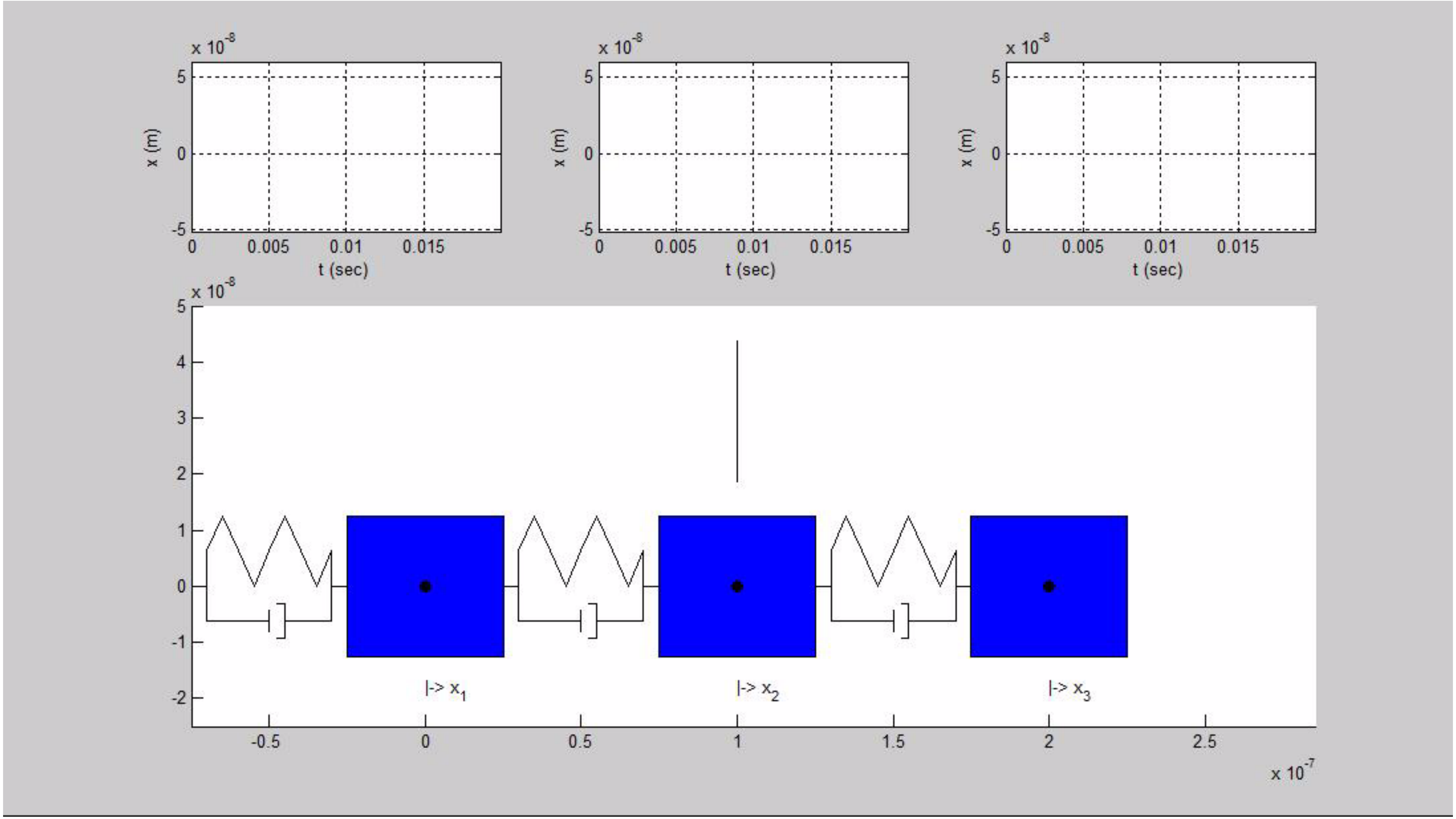

Discrete-time Transfer Matrix Method (DT-TMM)

- Example: 5-Mass System Control

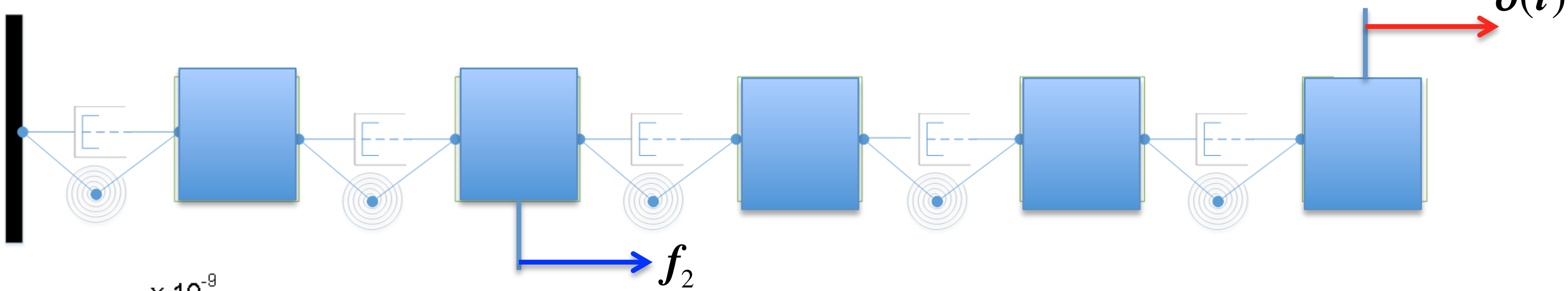

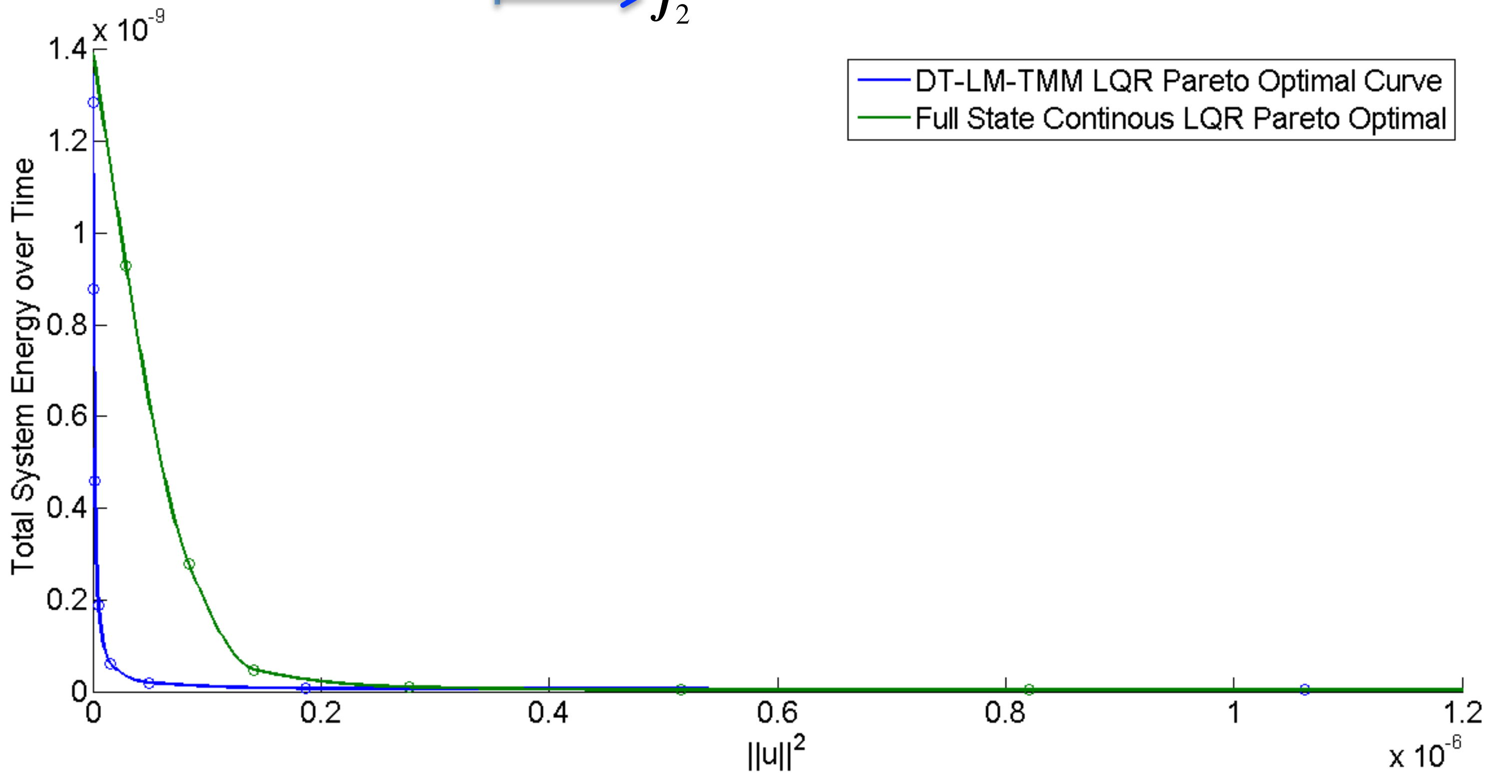

Discrete-time Transfer Matrix Method (DT-TMM)

- Example: 5-Mass System Control

Full-state continuous LQR

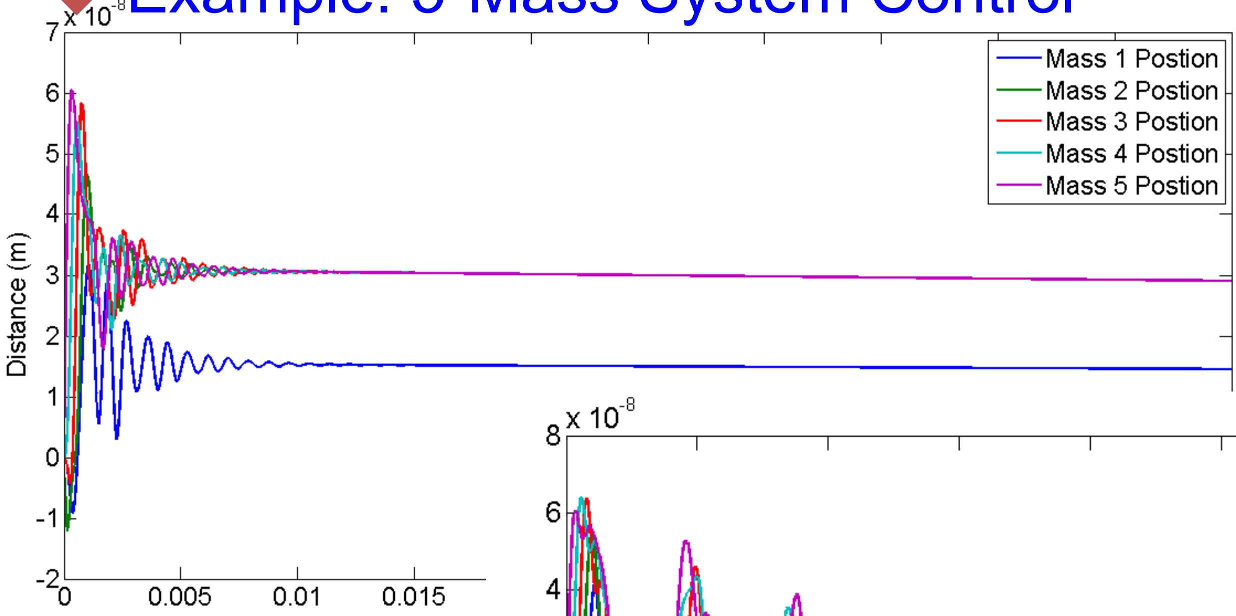

DT-TMM LQR

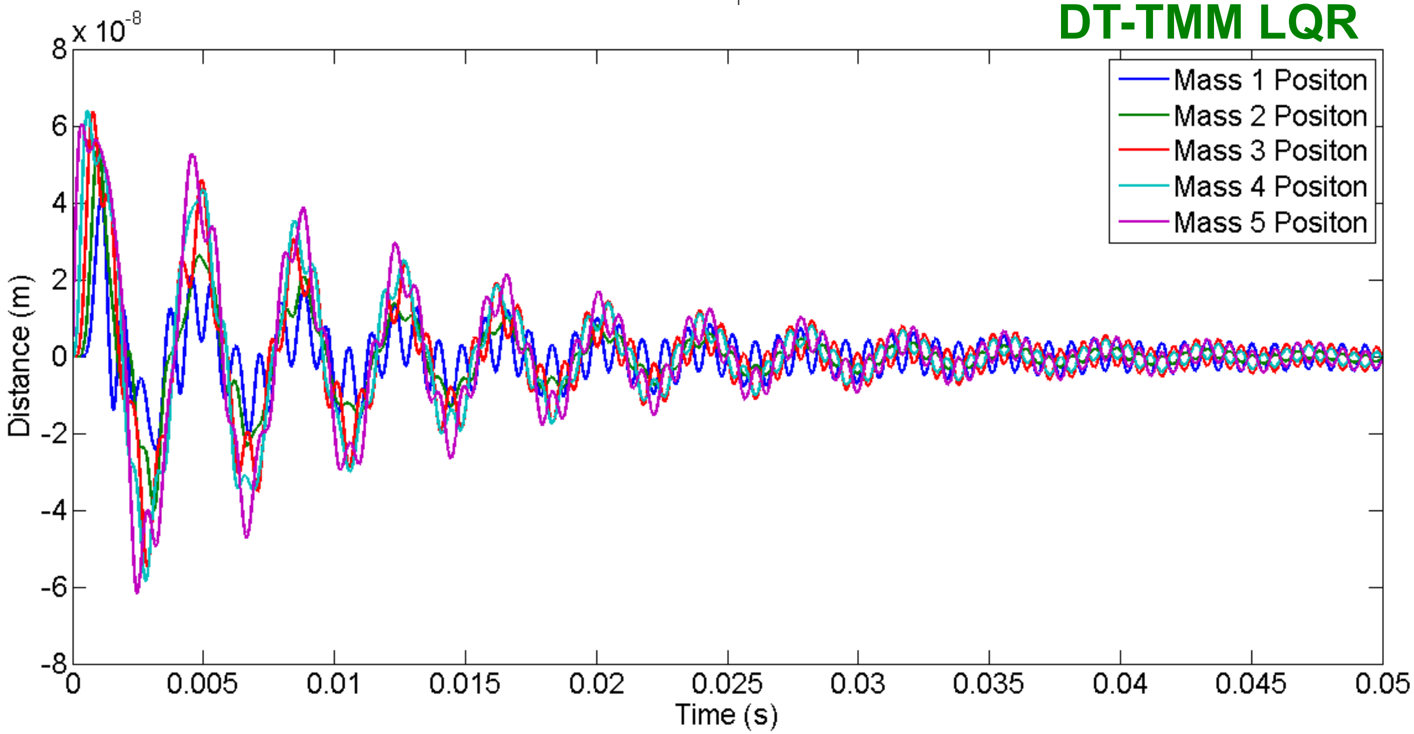

Modeling and Control of Lattice Structures

◆ Example: 5-Mass System Control (Continuous-Time LQR)

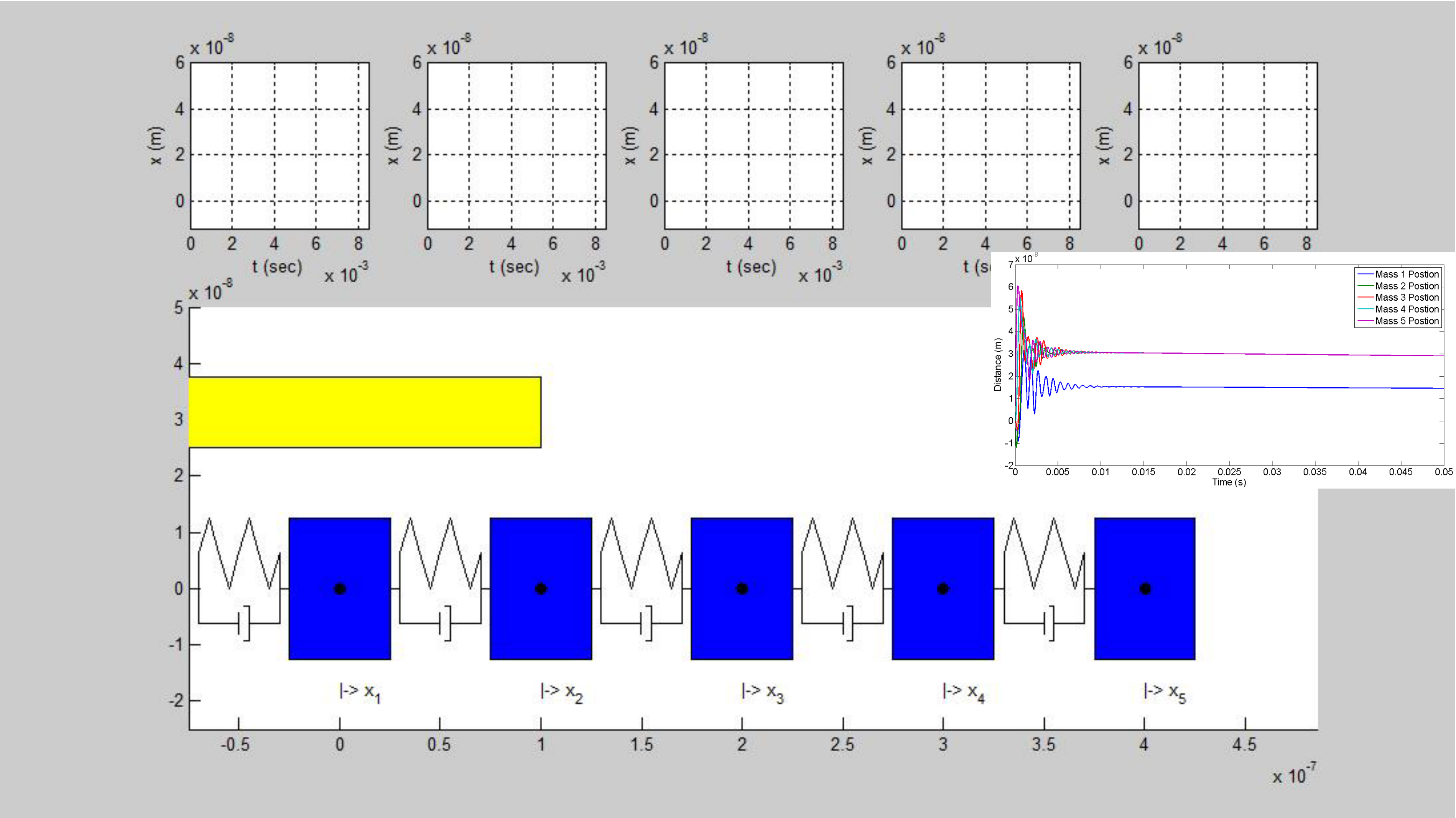

Modeling and Control of Lattice Structures

- Example: 5-Mass System Control (DT-TMM LQR)

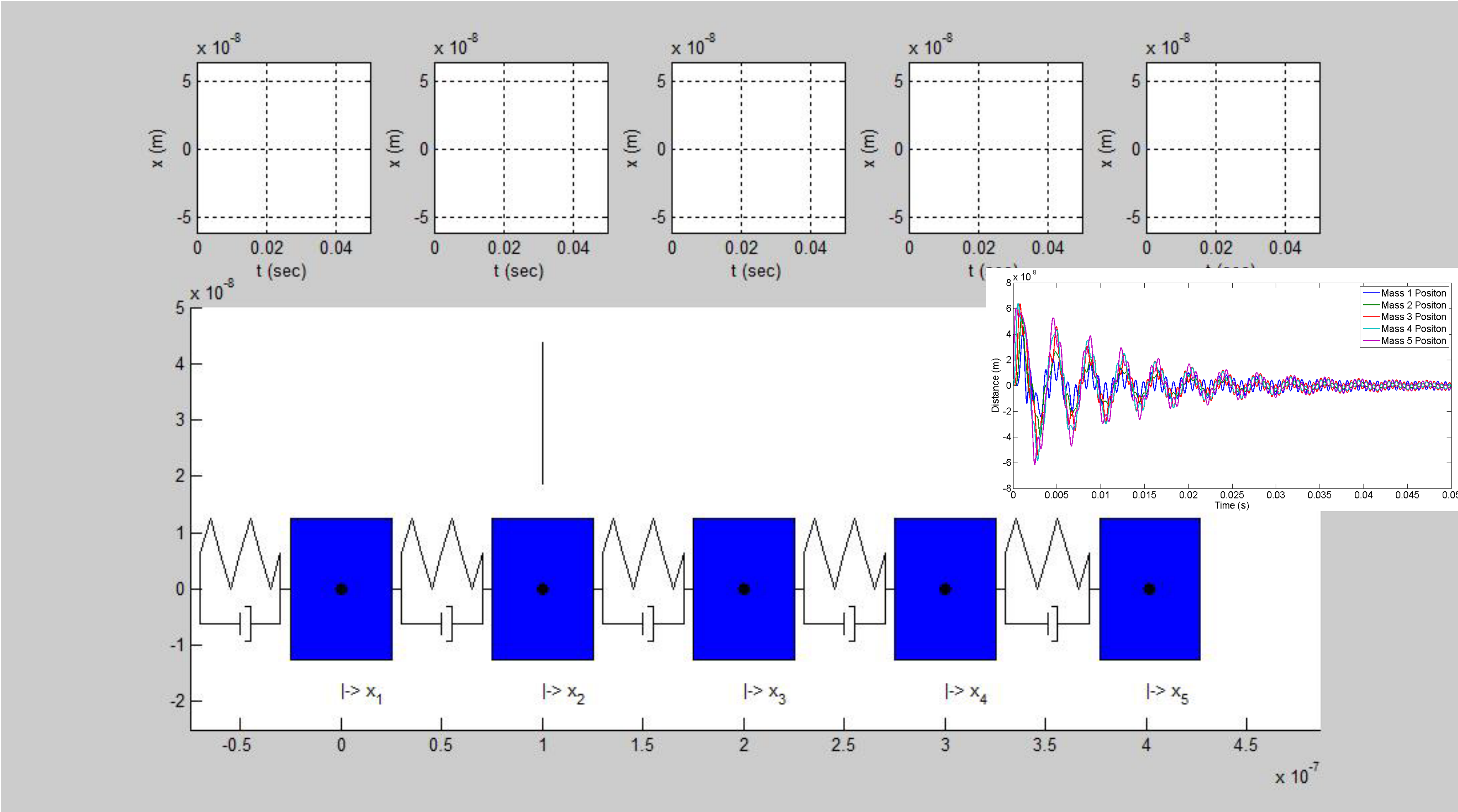

Summary

- Utilized lumped-mass approximation to model the lattice structures
- Through recursive application of discrete-time transfer matrix method, a localized reduced-order model was attained
- Houbolt numerical integration scheme was proposed, which allows for tuning the level of coupling from neighboring elements
- LQR-based decentralized controller was proposed, and it was used to effectively suppress vibrational behavior

Wind Tunnel Testing of Digital Wings

Team Members

LaRC

Mike Fremaux
Mark Croom
Emilie (Mia) Siochi
Wes Oneal
Clinton Duncan
Lee Pollard
Earl Harris
Sue Grafton
Gary Wainwright

ARC

Nick Cramer (UCSC)
Benjamin Jenett (MIT)
Daniel Cellucci (Cornell)
Kenny Cheung
Sean Swei

Wind Tunnel Tests: Overview

- One rigid and two flexible models of the digital structural design were created to explore the viability of the concept
- Two wind-tunnel investigations (MIT and LaRC 12-Ft Low Speed Tunnel) demonstrated the suitability of the wing concept against a range of environments:
  - Flight-like distributed loads
  - Aerodynamic performance
  - Flight control effectiveness

Wind Tunnel Tests: Key Findings

- Digital structure easily withstood aero loading across typical UAV flight envelope
  - dynamic pressures up to 7 psf (10 Pa)
  - speeds up to 77 fps (23 m/s)
  - thru post-stall angles of attack (>16˚)
  - moderate sideslip angles (generally only ±4˚, limited to 16˚)
- Digital structure at neutral twist exhibited similar aero properties as rigid variant in performance and static stability and roll-damping
- Flex structure allows for improved control options to enhance efficiency as compared to conventional design
- Controls-active tests demonstrate viability of digital structure active twist response dynamics against realistic loads and states

Models: Wing (+ Fuselage)

- Simplistic UAV platform component for this proof-of-concept study
- Flex and Rigid are geometrically identical
  - except for flap

Flexible twist Cont. variable	Rigid flaps Separate parts
-6˚ T.E. up to +10˚ T.E. down	0, ±10˚, ±20˚, ±30˚ both sides

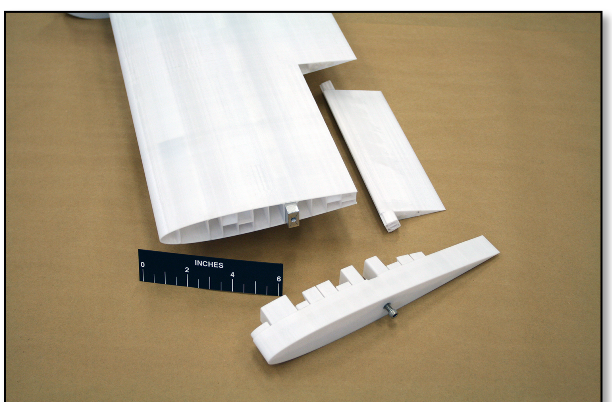

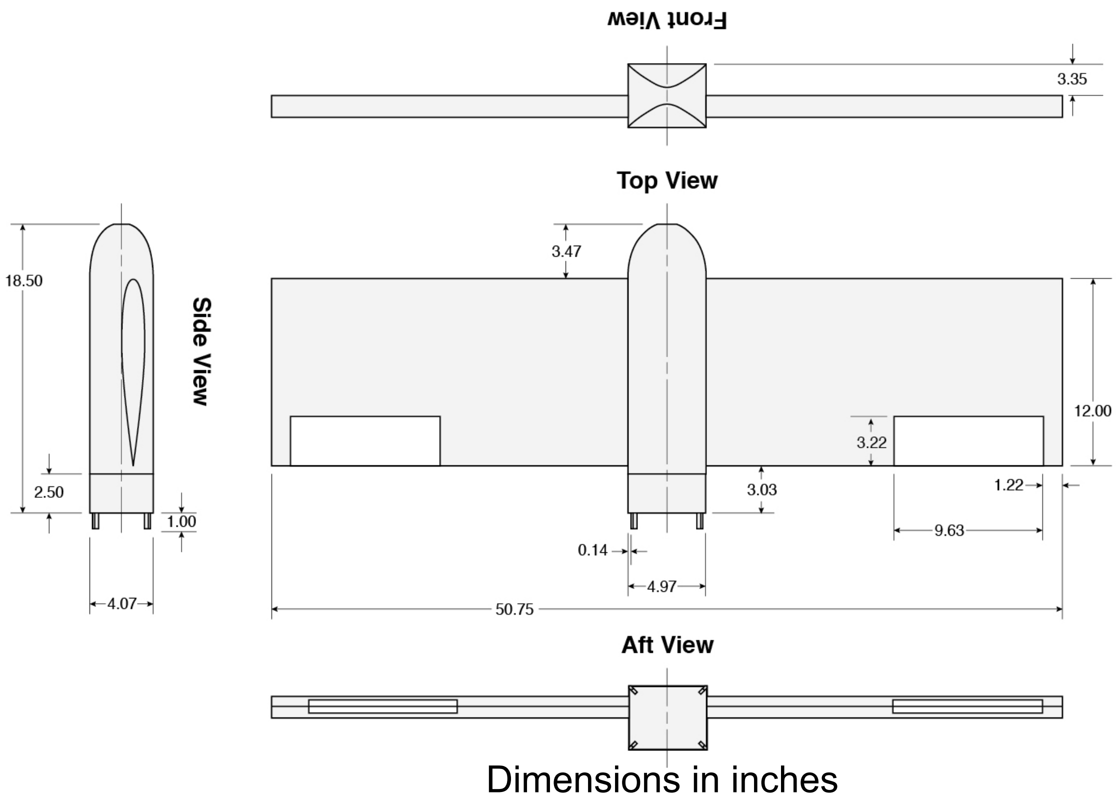

Rigid Model vs. Flex Model

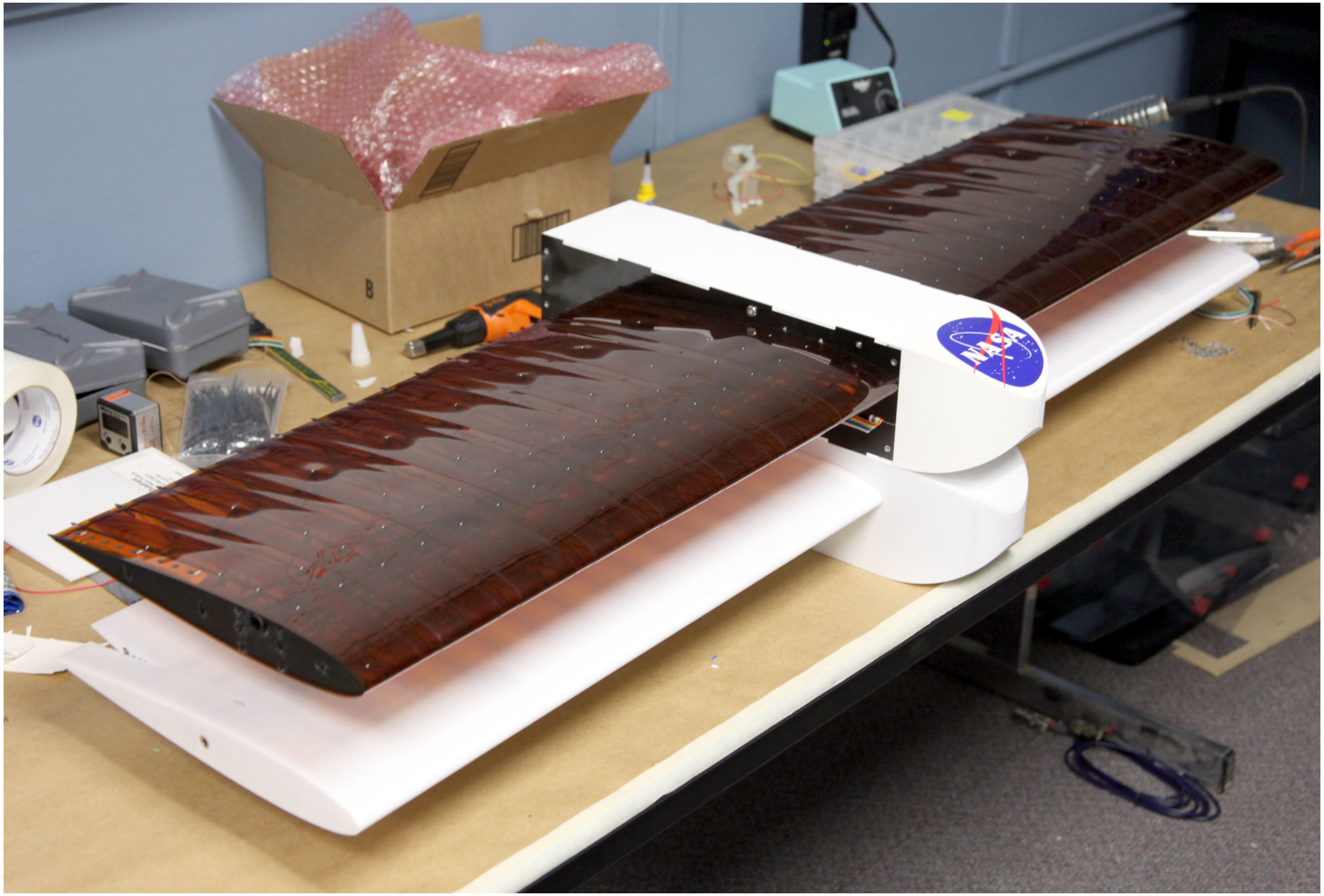

12-Foot Low Speed Tunnel

Specifications

- Type: Atmospheric, closed throat, annular return
- Test section: 8 sided, 12 feet wide, 15 feet long
- Operational: 1939 (as free-flight tunnel)
- Motor: 280 hp
- Velocity: 0 - 77 ft/s
- Static force and moment: -10 to 90 degrees alpha, +/- 90 degrees beta
- Surface pressures
- Arbitrary motion forced oscillation
- Free-to-roll
- Flow visualization (laser light sheet, tufts, smoke, sublimating chemicals

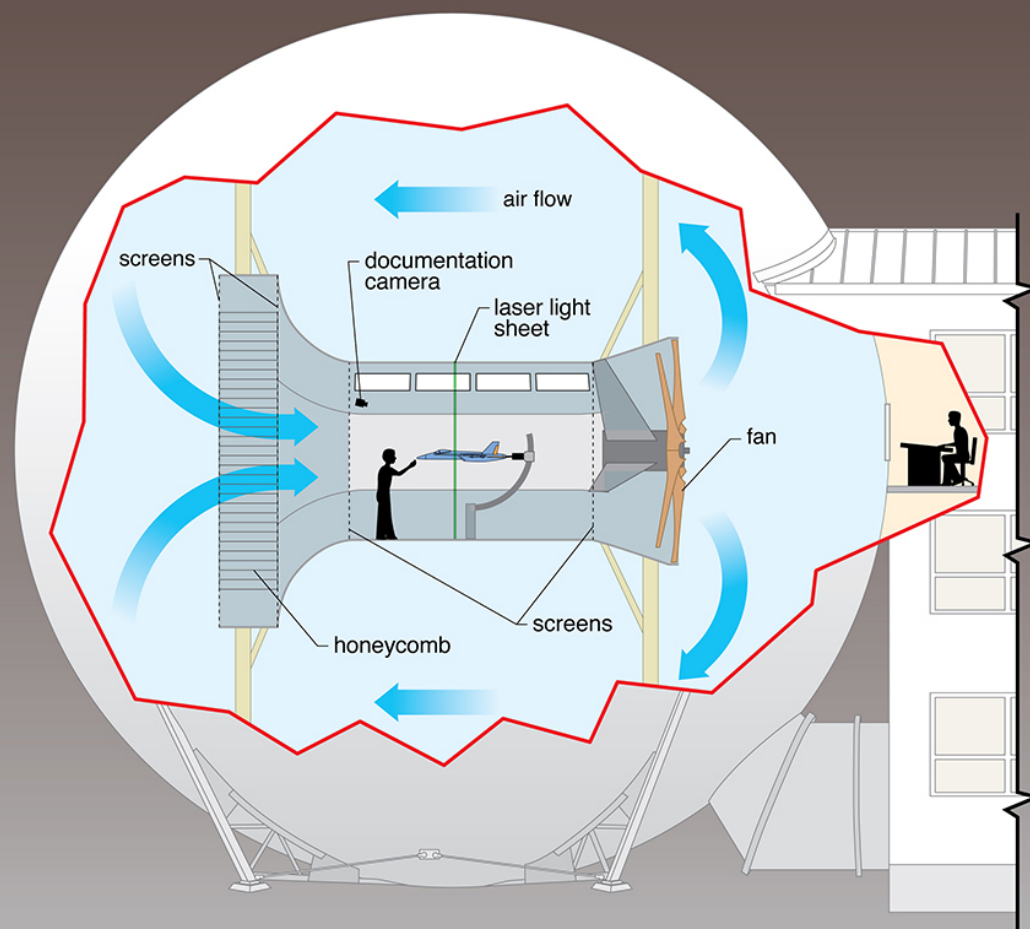

Models Installed in 12-Ft LST

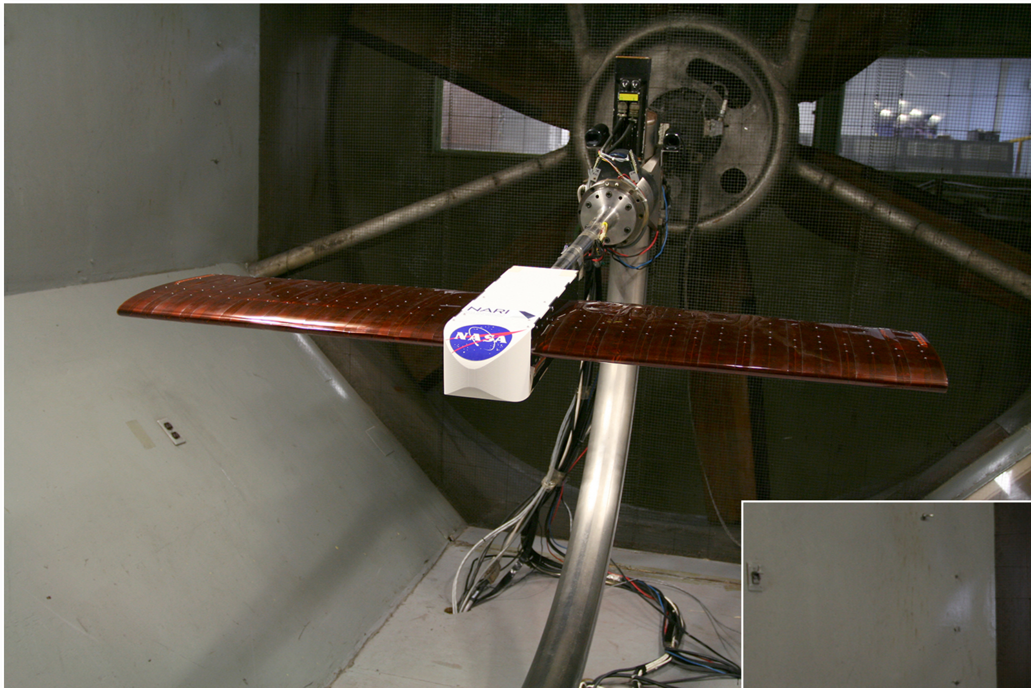

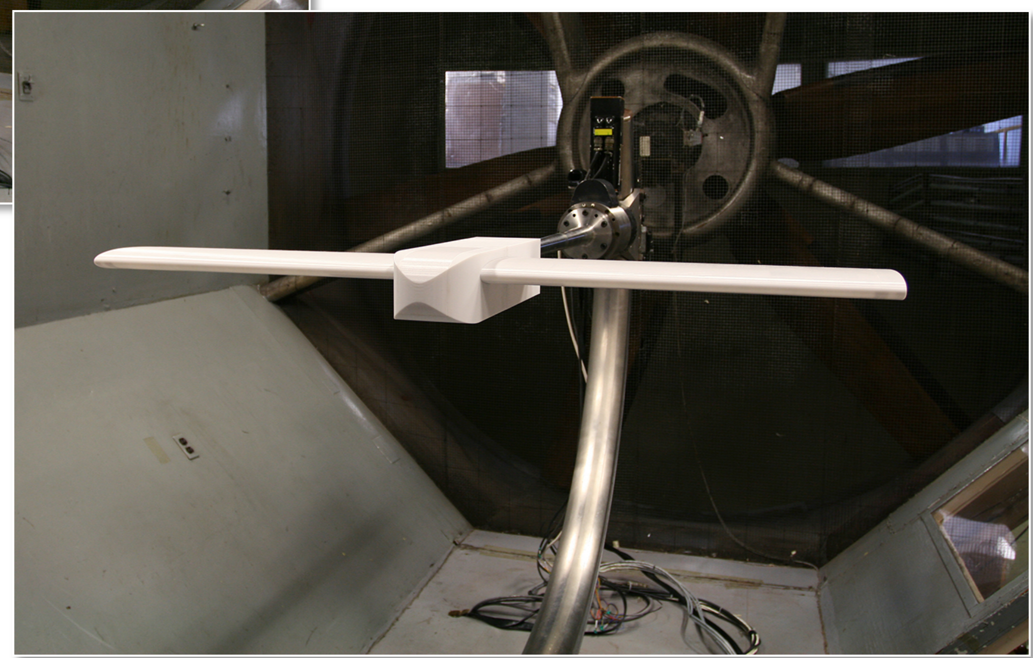

Comparisons – Longitudinal Aero

- Flexible shows similar levels of lift & drag as Rigid
- Both exhibit similar pitch static stability (Cm_{α}) levels
- ***Flex has ability to modulate the forces while maintaining trim more so than Rigid***

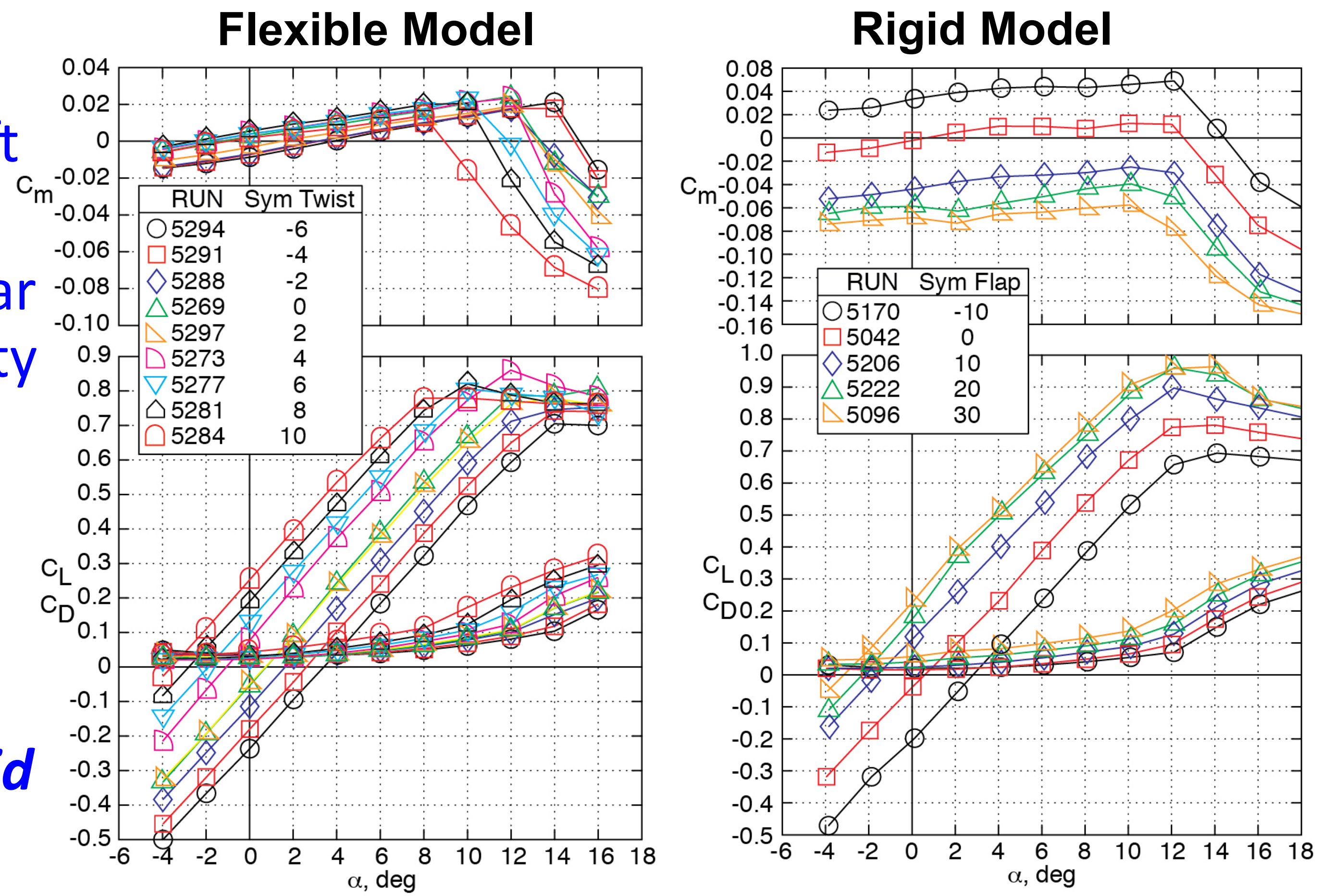

Comparisons – Pitch Control

- Using twist as a pitch controller on the Flex design shows potential for improved efficiencies
- ***Flex provides increased lift with reduced drag compared to the conventional flap in the pre-stall regime***
- Flex requires minimal balancing forces to maintain trim
  - Influenced by design approach

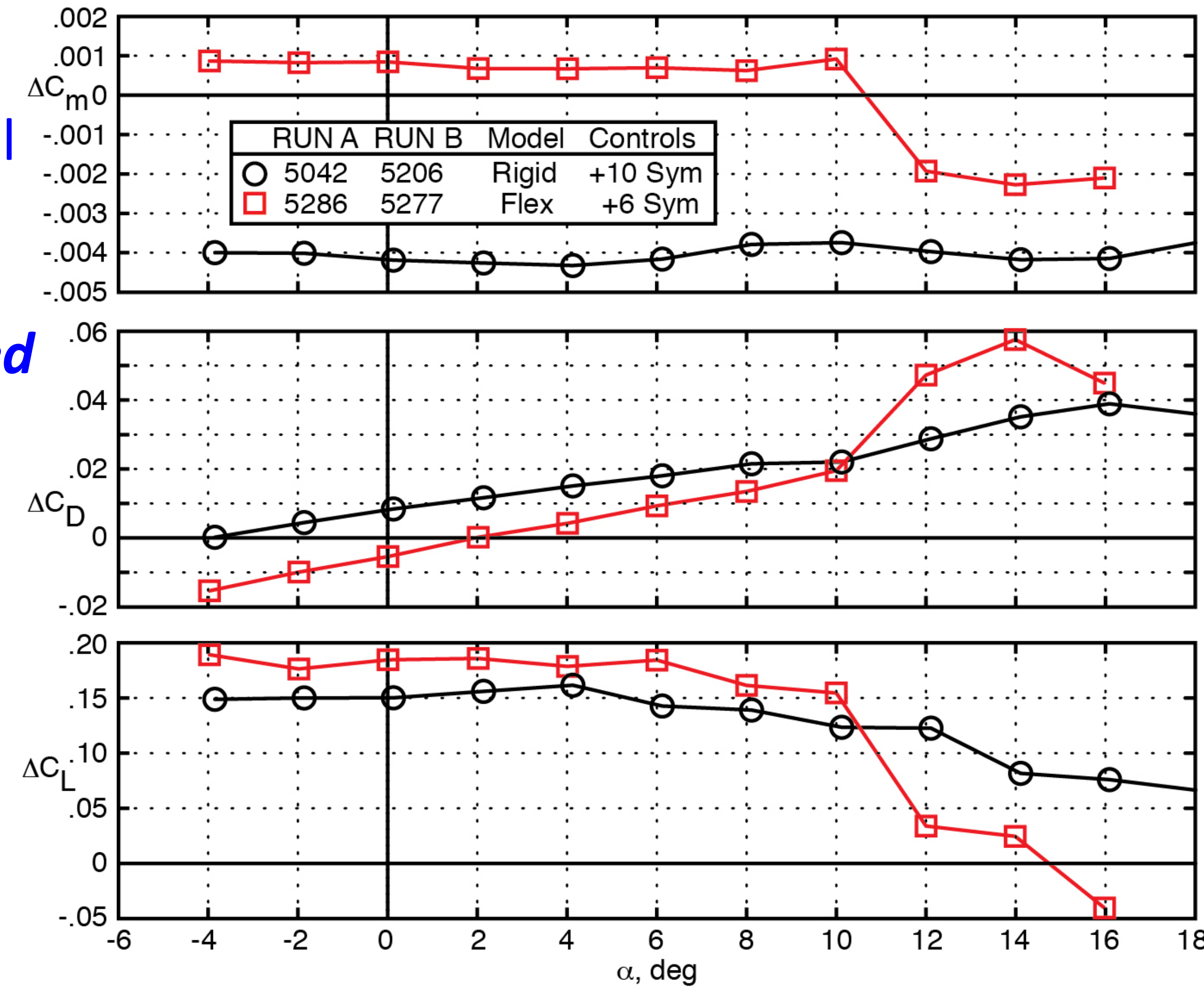

Lateral-Directional Static Stability

- Effective dihedral angle is stable (negative $C_{l\beta}$) as aoa increases
- Low levels of directional stability (wing only)
- Similar trends between Flex and Rigid (not shown)

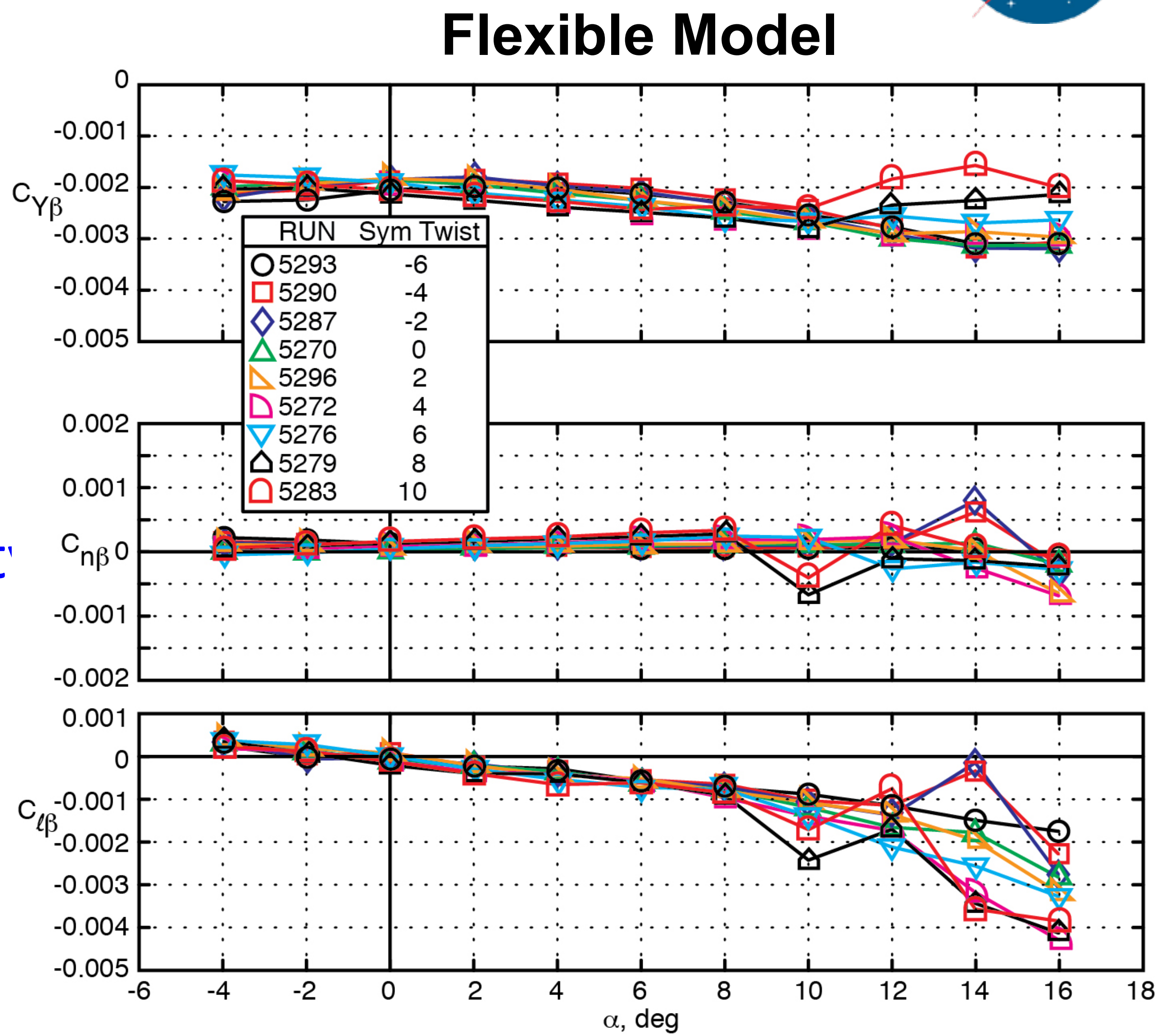

Comparisons – Lateral Control

- Twist is an effective static lateral (roll) controller
  - "weighted per area" effect is similar to differential flaps
- Post-stall: twist roll control degrades and brings on more pronounced coupling yawing moments
  - Twist can be further tailored to reduce yaw onset at post stall using non-zero average

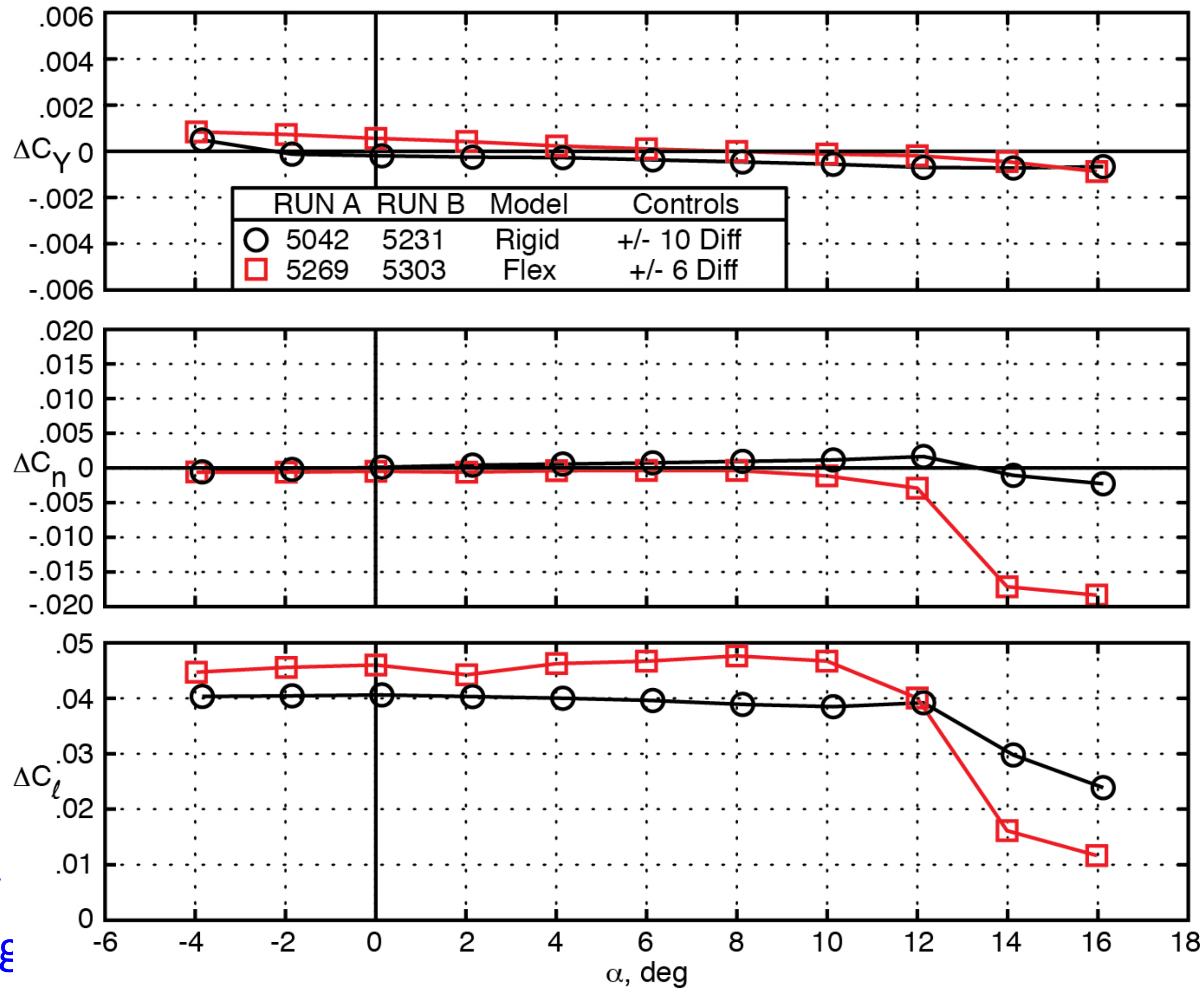

Comparisons: Roll Damping

- Flex and Rigid show nearly identical classic roll forced oscillation rate derivative levels
  - Across aoa, freq, amp variations tested
  - Controls fixed
  - Wing component provides suitable levels of roll damping

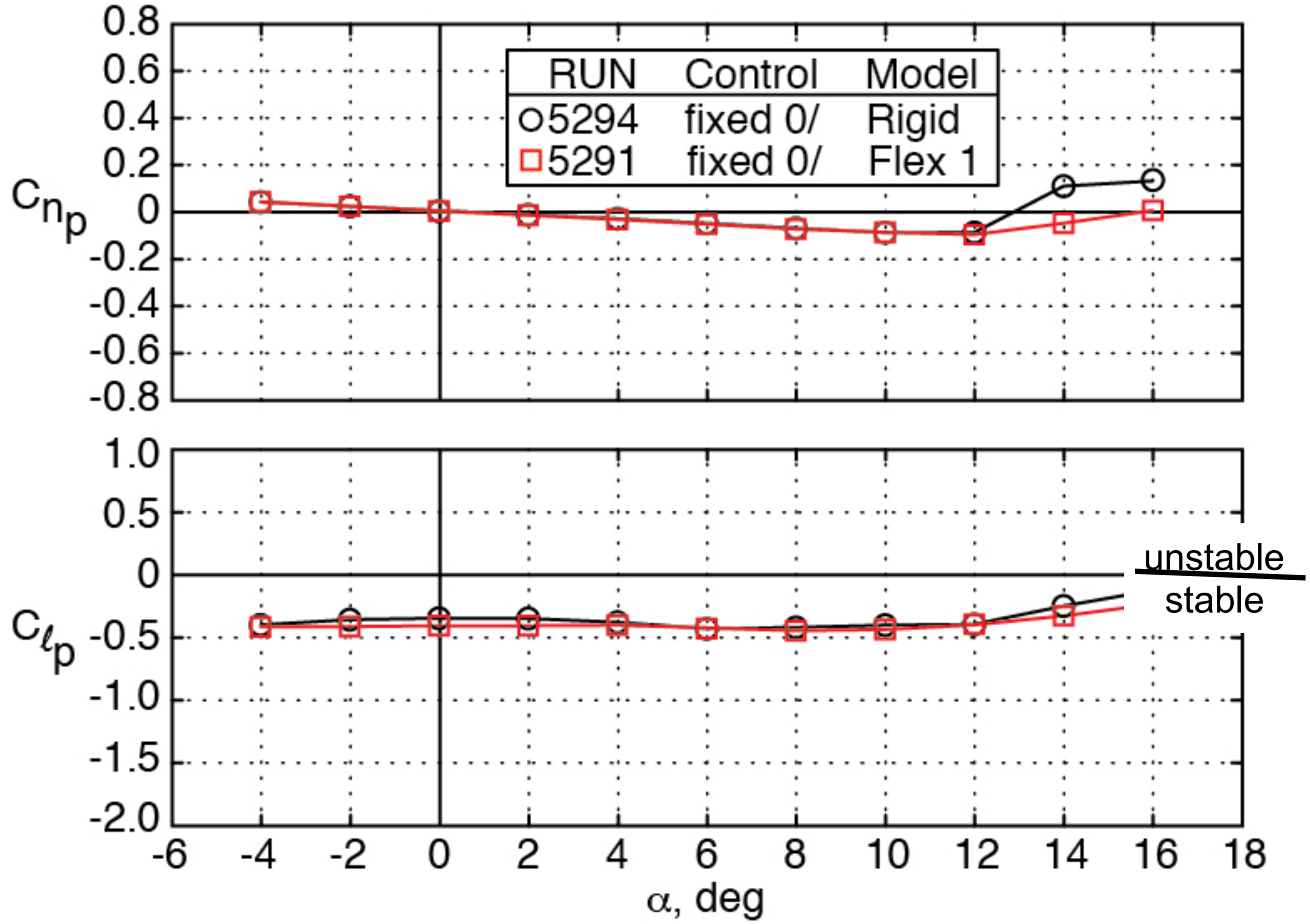

Damping Augmentation

- Wing twist commanded in response to the sensed model motion
  - Drive controls in-phase and out-of-phase, and quadrature wrt sensed bank angle
    - Stabilizing and destabilizing influences with rate and angular position
    - Classic roll damper (Rt = +p)
  - Experimentally demonstrate efficacy against uncertainties in the control flow
  - Lightweight wing structure is advantageous from a testing standpoint (dynamic tares)

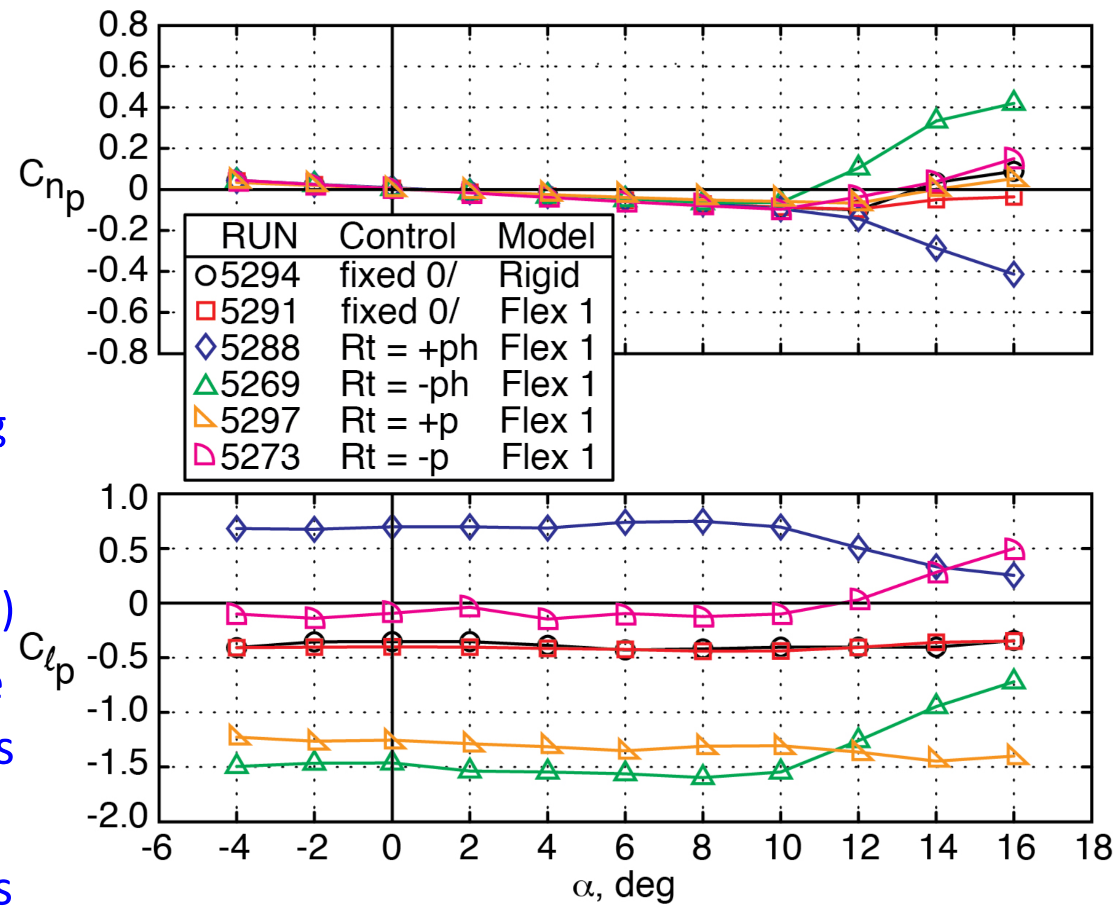

Dynamic Controls

- Analyses of force and moment time-histories collected at a set condition (fixed AoA, qbar) indicate twist oscillations hold potential for performance improvements

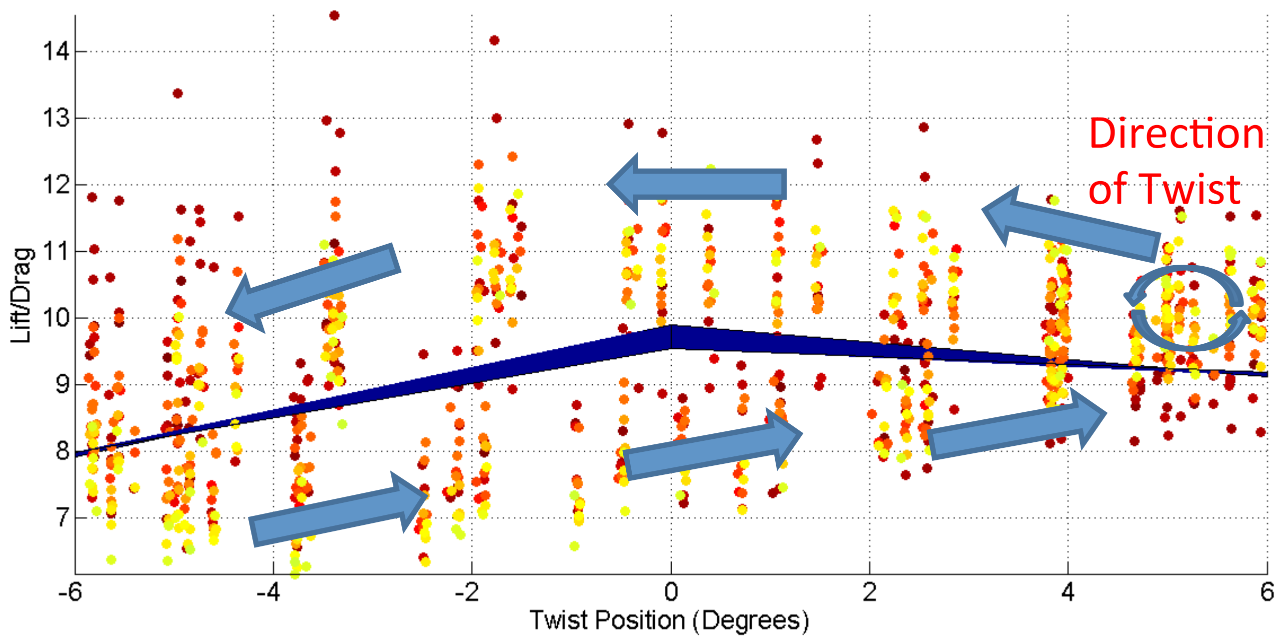

Oscillation around certain twist can improve performance!

Wind Tunnel Tests: Animations

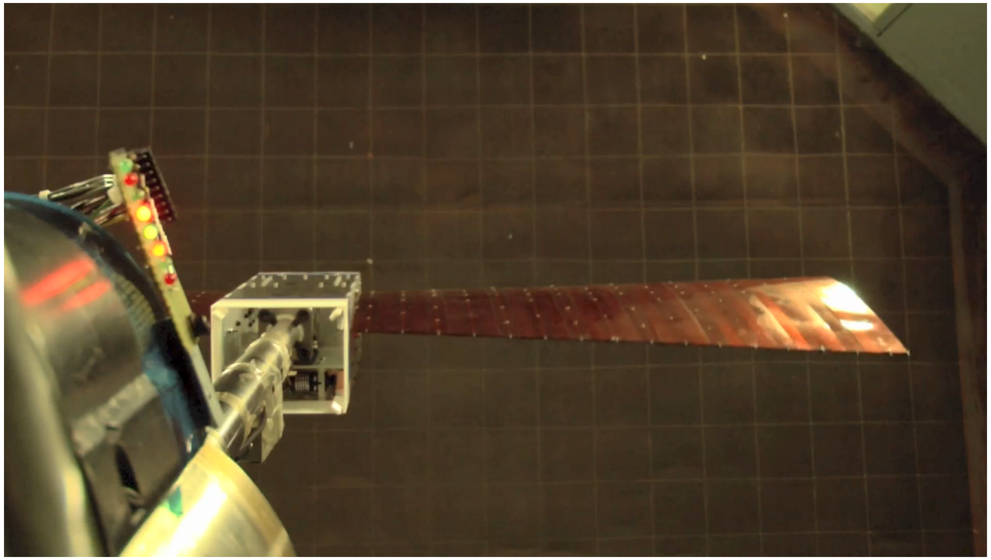

- Flutter suppression tests
  - High AoA
  - Stabilized via wing tip twist

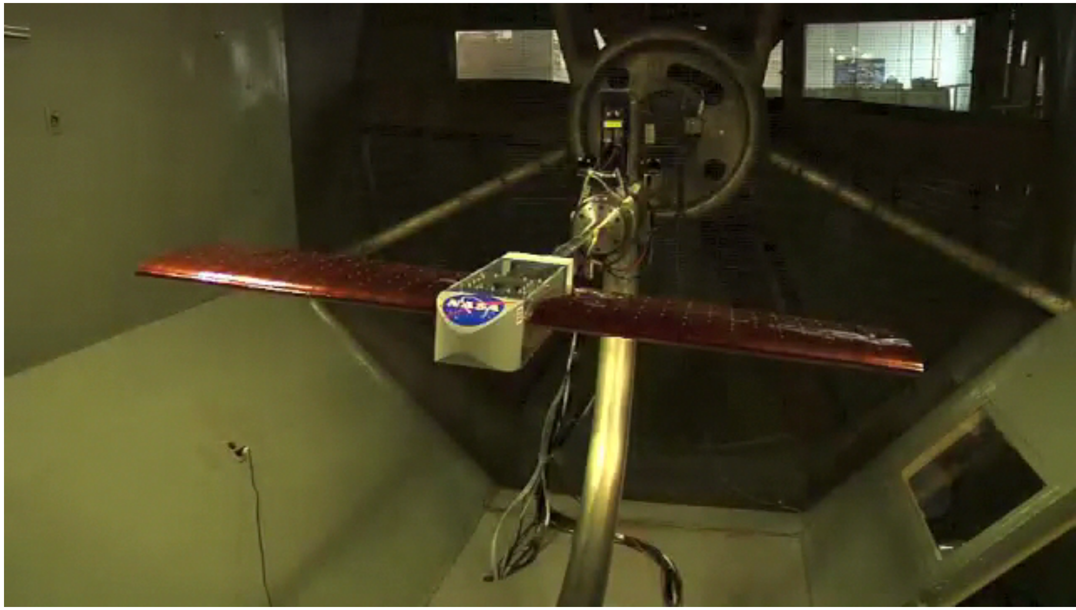

- High frequency morphing
  - Free roll
  - Can vary wing twist frequency

Summary

- Digital structure approach provides classic stable and controllable wing attributes across general low-speed small UAV operating envelope of AoA, speed, sideslip and control
  - Structurally and aerodynamically
  - Statics and dynamics
- Modulating twist can improve efficiencies of overall vehicle design
- Closed-loop tests demonstrate effectiveness of the realistic actuator-to-fluid control "system"
- **Continued studies**
  - **Bring in additional total-vehicle components (horizontal and possibly vertical surfaces/controls)**
  - **Include on-surface flow measurements; additional controller dynamics**
  - **Exploit aerodynamics (vehicle structure, controls, and ensuing motion) for enhanced performance/efficiencies**

EXECUTIVE SUMMARY

NARI
NASA AERONAUTICS RESEARCH INSTITUTE

NASA

Executive Summary

- Design and fabrication of wing structures utilizing lattice-based construction approach, with limited number of distinct components
- A novel transfer matrix approach to model and control the dynamics of lumped-mass behaviors of interconnected cellular components
- Through rigorous best tests and wind tunnel tests, the proposed lattice-based flexible wing structures proved to behave as conventional wing design, but with added versatilities that could enable new mission objectives

PLAN FORWARD

Plan Forward

- Development of Physical Finite Element Model (PFEM) analysis technique
- Lattice structural modal identification and validation
  - System ID process
  - Structural properties
- Flexible PCB for onboard, real-time, flow sensing
- Mission adaptive wing shaping to improve in-flight aerodynamic performance

dwc238@cornell.edu

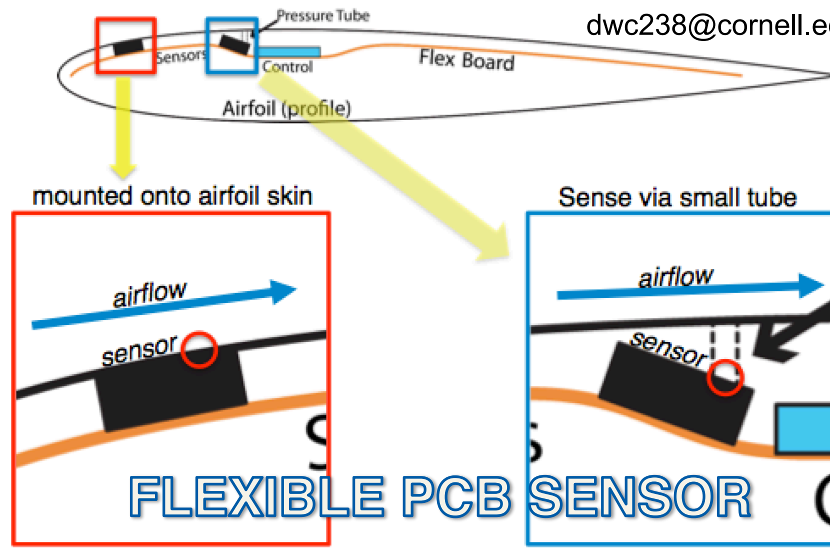

PHYSICAL FINITE ELEMENT MODEL

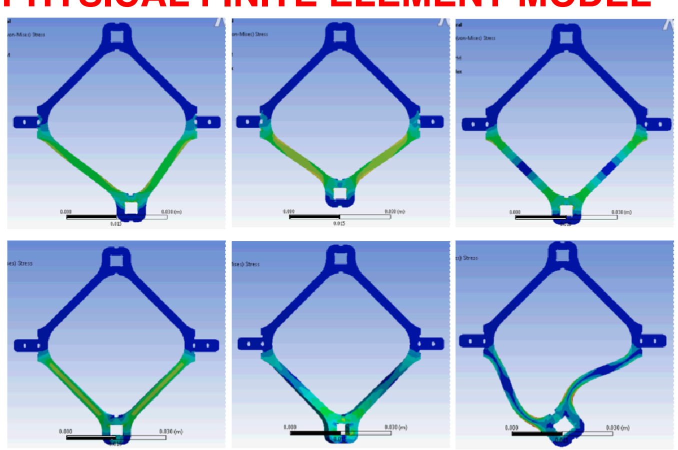

sam.calisch@cba.mit.edu

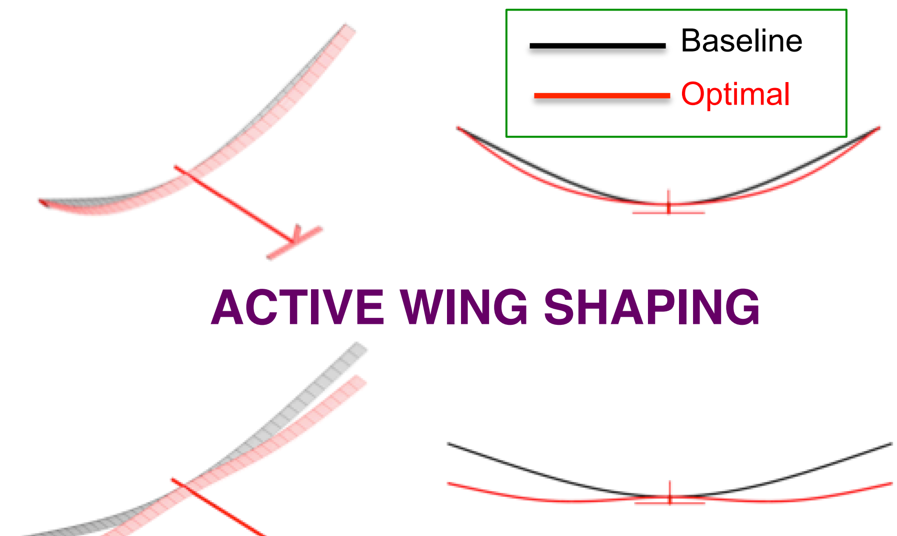

suw@eng.ua.edu

Plan Forward

- Wind tunnel tests with total-vehicle components (horizontal and possibly vertical surfaces/controls)
- Development of robotic assembly and repair capability
- Large scale shape morphing-based propulsion that enables the flapping wing flight

NASA AERONAUTICS RESEARCH INSTITUTE

Thank you!

Question?

LaRC 12-ft Test Team – Thanks!